



Joint European Research Infrastructure network for Coastal Observatory –  
Novel European eXpertise for coastal observaTories - **JERICO-NEXT**

<b>Deliverable title</b>	Progress report after development of microbial and molecular sensors
<b>Work Package Title</b>	WP 3 Innovation in Technology and Methodology
<b>Deliverable number</b>	D3.7
<b>Description</b>	Progress report after development of microbial and molecular sensors
<b>Lead beneficiary</b>	IRIS
<b>Lead Authors</b>	Catherine Boccadoro (IRIS), Wilhelm Petersen (HZG), Bengt Karlson (SMHI), Florent Colas (Ifremer)
<b>Contributors</b>	Anne Vatland Krøvel, Mari Mæland Nilsen
<b>Submitted by</b>	
<b>Revision number</b>	2.0
<b>Revision Date</b>	06 Oct. 2017
<b>Security</b>	Public



The JERICO-NEXT project is funded by the European Commission's H2020 Framework Programme under grant agreement No. 654410  
Project coordinator: Ifremer, France.





History			
Revision	Date	Modification	Author
1.0	04 Oct. 2017	Complete version content added by all authors	Catherine Boccadoro
2.0	06 Oct 2017	First revision by all authors	Catherine Boccadoro

Approvals				
	Name	Organisation	Date	Visa
<b>Coordinator</b>	Farcy Patrick	Ifremer	12 octobre 2017	PF
<b>WP Leaders</b>	Petihakis George Delauney Laurent	HCMR Ifremer	10 octobre 2017	

## PROPRIETARY RIGHTS STATEMENT





THIS DOCUMENT CONTAINS INFORMATION, WHICH IS PROPRIETARY TO THE **JERICO-NEXT** CONSORTIUM. NEITHER THIS DOCUMENT NOR THE INFORMATION CONTAINED HEREIN SHALL BE USED, DUPLICATED OR COMMUNICATED EXCEPT WITH THE PRIOR WRITTEN CONSENT OF THE **JERICO-NEXT** COORDINATOR.





## Table of contents

1	Executive Summary .....	5
2	Introduction .....	6
2.1	Speciation through 16SrRNA and 18SrRNA gene sequencing .....	6
2.2	Task objectives.....	6
3	Microbial molecular markers for pollution detection .....	8
3.1	Selected assays for coastal seawater monitoring .....	8
3.2	Seawater sample collection for marker and assay development and testing .....	9
3.2.1	Environmental sampling.....	9
3.2.2	Samples collected through different experimental set ups for marker testing and selection.....	10
3.2.3	Cruise sample collection in conjunction with WP4 JRAP3 .....	11
3.3	Preliminary results on assays and marker robustness .....	11
3.3.1	Total number of bacteria assay.....	11
3.3.2	Assay for total number of Colwellia organisms .....	12
3.3.3	Assay for the quantification of Oleispira antarctica organisms.....	13
3.3.4	Assay for the quantification of Alteromonas, Marinobacter, Alcanivorax (AMA) organisms.....	14
3.4	Preliminary conclusions from assays .....	15
4	Metabarcoding - a tool for investigating plankton diversity and harmful algal blooms.....	16
4.1	Introduction to metabarcoding of plankton .....	16
4.2	Preliminary results.....	17
4.2.1	Ferrybox samples .....	17
4.2.1	About preservation of samples for rDNA analyses of plankton.....	25
4.2.2	A harmful algal bloom study at Tångesund, Swedish west coast .....	25
5	Biosensors for the detection of toxic algae .....	26
5.1	Detection of toxic algae through nucleic acid detection.....	26
5.2	Development of an in-situ optical sensor for the detection of toxins.....	28
5.2.1	SPRi sensors: .....	29
5.2.2	Design of the SPRi sensor:.....	32
5.2.3	Detection protocol optimisation: .....	39
6	Preliminary conclusions and further work .....	42
7	References.....	43





## 1 Executive Summary

The aim of Task 3.4 is to develop and test innovative methods for the molecular detection of phytoplankton, harmful algal blooms and pollutants through their effect on microbial communities. This will include the development of novel molecular sensors for the detection, quantification and identification of organisms, microbial markers of pollutant exposure or toxin concentrations in marine coastal waters.

Bacterial species and genes which can be used as markers of high nutrient load or hydrocarbon contamination in the marine environment were identified through bacterial community analysis in contaminated environment and literature reviews. Assays using quantitative Polymerase Chain Reaction (qPCR) for the quantification of these organisms were developed and tested through environmental sampling campaigns and laboratory exposure studies. The most promising markers and assays were selected for further study in conjunction with other biological and chemical sensors, and will be further tested through campaigns to be performed through WP4.

Complementary technologies are being developed through this task to monitor toxic algae, combining an approach based on the detection of the organisms through an autonomous sensor, and the detection of toxins using a probe. The fully automated sensor module for autonomous monitoring of toxic algae includes a remote-controlled automated filtration system coupled to a semi-automated nucleic acid biosensor based on the specific binding of a molecular. This sensor will be adapted and optimised for long term unattended operation on Ferrybox systems through this task. In parallel, for the direct detection of algae toxins, the capabilities of an *in situ* optical biosensor were extended. This was done to reduce the device size, increase its efficiency, and potentially extend its performance to detect more than domoic acid, which was the toxin that the sensor was initially designed for. In this first phase of the project, the sensor was successfully redesigned and is planned to be tested in laboratory conditions prior to deployment at sea.

For investigating plankton diversity and harmful algal blooms rDNA meta barcoding methods were developed and evaluated by analyzing samples collected using a Ferrybox system in the Baltic Sea area. Results based on 16S and 18S rDNA show that metabarcoding reveals a much higher diversity in phytoplankton compared to microscopy. However, metabarcoding only gives results on relative abundance of genes (OTU, Operational Taxonomical Units) in samples and does not give information about biomass. Microscopy gives cell numbers and biomass based on cell volumes. The two different approaches complement each other. Metabarcoding is being further evaluated through comparison with *in situ* imaging flow cytometry and microscopy in a study of harmful algal blooms on the Swedish Skagerrak coast.

**This progress report includes the work performed during the first two years of the project. During this first phase of the project, much of the focus has been on the development and improvements of the different types of sensors and biosensors before the sensor testing through laboratory and field campaigns, which will involve sensor tests in a common setting and integration of the results and responses from the different devices and tools.**





## 2 Introduction

The overall objective of Work Package 3 is to enhance the capability and the quality of measurements from the different coastal monitoring infrastructures in JERICO-NEXT, focusing on the biological measurements of the ecosystem. In JERICO-NEXT, several different approaches are used to improve observations of bacteria and plankton. In Task 3.1 the focus is optical methods, e.g. imaging in flow methods and detection of phytoplankton pigments by measuring bulk optical properties using fluorometry or spectrophotometry. Molecular methods used in WP3.4 may complement the other methods, giving detailed information of organisms at the gene level.

### 2.1 Speciation through 16SrRNA and 18SrRNA gene sequencing

The 16S ribosomal RNA (rRNA) gene that encodes for the 30S small subunit of prokaryotic ribosome is highly conserved and can be used for the construction of phylogenies (Woese and Fox, 1977; Woese et al., 1990). Sequencing of the variable regions of the gene can provide species-specific identification of bacteria. 18S rRNA is the eukaryotic nuclear homologue of 16SrRNA in prokaryotes. It is a component of the small eukaryotic 40S ribosomal subunit and its gene is often used in phylogenetic studies (Meyer et al., 2010). In this work, these are used for the speciation of bacteria, archae and phytoplankton, for environmental biodiversity screening, and for detection or quantification of particular species or genera.

### 2.2 Task objectives

The aim of Task 3.4 is to evaluate and develop methods for the molecular (i.e. gene based) detection of phytoplankton, harmful algal blooms and pollutants through their effect on microbial communities. In addition, novel platforms and sampling methods to accommodate these technologies will be evaluated. This work includes the development of novel molecular sensors for the detection and identification of organisms, microbial markers of pollutant exposure or toxin concentrations. The molecular sensors can be adapted to existing platforms to incorporate biological parameters into existing measurement platforms. Task 3.4 is divided into three subtasks:

#### SubTask: 3.4.1 Microbial molecular markers for pollution detection

This subtask involves the identification of suitable microbial marker genes and species, and development of assays for monitoring microbial organisms linked to hydrocarbon pollution in coastal seawater using quantification of particular genes and species through quantitative Polymerase Chain Reaction (qPCR).

#### SubTask: 3.4.2 Biosensors for the detection of toxic algae

This subtask aims to extend the capabilities of *in situ* biosensor for algae toxin. Ifremer has previously developed an optical biosensor for the detection of domoic acid (DA), a neurotoxin produced by some *pseudo-Nitzschia spp.* This biosensor was demonstrated capable of assaying DA at concentration levels as low as 0.1 ng/mL in operational conditions, and the first result was very promising. However, the system suffered from some limitations: reproducibility, stability for long term deployment, and cost-efficiency. In addition, the system was dedicated to only one toxin. The objective of this subtask is thus to overcome these limitations. A new sensor configuration has been studied, designed, and is being fabricated. The novel system will be tested in the laboratory and *in situ* during 2018. The potential use for the detection of other compounds will be studied as well.





SubTask: 3.4.3 Metabarcoding as a tool for investigating plankton diversity and harmful algae blooms

Through this subtask, rDNA metabarcoding will be tested in parallel with more traditional biodiversity studies to test its potential as a reliable and efficient method for monitoring biodiversity and presence of algae blooms.





### 3 Microbial molecular markers for pollution detection

Pollutant exposures in the marine environment trigger specific changes within microbial communities, resulting in some species and genes becoming much more prominent following contaminant exposure or environmental changes. Subtle microbial population shifts can be very informative about acute spills as well as chronic low levels of exposure, which can be extremely challenging to detect and quantify using more traditional chemical analysis. Such changes can be detected and quantified through qPCR analysis of seawater DNA samples, which may be obtained using existing coastal monitoring platforms. This task will develop the method, focusing on the identification of suitable marker organisms and genes for the detection of pollutants, with focus on chronic and acute low-level hydrocarbon pollution. The collection and preservation of samples will be adapted to the Ferrybox through Sub-Task 3.4.3.

In this initial phase of the project, the aim of the work was to select and test different microbial markers for the detection of hydrocarbon pollutants in coastal seawaters. A selection of microbial DNA candidate targets was made based on *a priori* knowledge from the literature and scientific experience. Both phylogenetic and functional target genes were selected, with emphasis towards genes and species involved in degradation of hydrocarbons in the marine environment. However, target genes related to other kinds of environmental challenges, such as seawater eutrophication and algae blooms, were also selected and tested in this preliminary phase.

#### 3.1 Selected assays for coastal seawater monitoring

Microbial markers are selected as particular detectable organisms or genes which are found in higher numbers within the seawater microbial community under particular environmental conditions or in the presence of contaminants. Once the appropriate targets are identified, assays for real-time quantification of the targets are developed and tested through laboratory exposures and selected environmental sampling in known pristine and contaminated areas. It should be noted that the water temperature, water chemistry (nutrients) and indigenous bacterial communities from various locations will influence the selection of optimal qPCR assays for monitoring studies, which is a challenge when the aim is to select 'universal' assays suitable for coastal monitoring in different geographical locations. Some targets are therefore selected markers for specific areas, climates and water depths, while others may be more generic. Detailed below are the different target marker species or genes which were selected to be tested for coastal marine monitoring, focusing on the detection of hydrocarbon contamination in the marine environment.

1. **Quantification of total number of bacteria (TNB)** using several universal primer sets which specifically detect 16S rRNA gene of the Domain Bacteria (Nadkarni et al., 2002).
2. **Quantification of total number of Archaea (TNA)** using a universal primer set which specifically detects 16S rRNA of the Domain Archaea (Takai and Horikoshi, 2000).
3. **Quantification of Hydrocarbon degrading organisms:**  
*Oleispira Antartica*. This hydrocarbonoclastic bacterium has been shown to be an important oil degrading microorganism in cold marine environments (Yakimov et al., 2003; Krolicka et al., 2014; Boccadoro et al, In prep). The total number of these organisms in an environmental sample





is estimated using a primer set which specifically detects the small subunit of the ribosomal gene (16S rRNA) of *O. Antarctica* (Krolicka et al., 2014).

***Colwellia***. These species have been reported to be capable of degrading hydrocarbons, including during the Deepwater Horizon oil spill in 2010 (Redmond and Valentine, 2012; Mason et al., 2012). *Colwellia* species play also a role in global carbon and nutrient cycling in cold marine environments (Deming, 2002). Primer sets were designed for the quantification of these organisms (Krolicka et al., 2014).

***Alteromonas, Marinobacter, Alcanivorax (AMA)***. Primers were designed to quantify these typical marine hydrocarbonoclastic microorganisms in the marine environment (Krolicka et al., 2014).

#### 4. Quantification of hydrocarbon degrading genes:

AlkB and catA are genes that encodes for key enzymes involved in bacterial hydrocarbon degradation; **alkane monooxygenase** (alkane degradation) and **catechol-2,3-dioxygenase** (aromatic hydrocarbons), respectively. Primers were designed to quantify these genes (Knapik et al, In prep).

### 3.2 Seawater sample collection for marker and assay development and testing

#### 3.2.1 Environmental sampling

Seawater samples were collected at various depths from different geographical locations. Samples were collected in pristine coastal areas as well as areas of heavy industrial traffic, such as harbours and heavily contaminated areas close to industry discharges. In addition, samples were collected in close proximity to aquaculture farming areas, as described in Table 3.1.

Table 3.1: Descriptions of environmental samples

Name of sample	Description
Harbor low	Seawater sampled from the surface water (approximately 0.5-1 m depth) in the port of Mekjarvik in January 2017, which is expected to be contaminated with petroleum compounds. This harbour is the terminal for the Mekjarvik-Kvitsøy ferry, with 8-10 departures each day. The sampling site is located approximately 100-200 meters away from where the ferry departs, and is expected to be contaminated by only low levels of hydrocarbons.
Harbor medium	Seawater sampled from the surface water (approximately 0.5-1 m depth) in the port of Mekjarvik (described above), in January 2017. The ferry departs from the right side of the pier, and this sampling location is situated on the left side of the pier in the port.
Harbor high	Seawater sampled from the surface water (approximately 0.5-1 m depth) in the port of Mekjarvik (described above), in January 2017. This sampling location is situated on the same side of the pier as the ferry departs from. Samples were





	collected 5-10 minutes after departure of the ferry and are expected to be the most oil contaminated samples from this region. Sampling site exhibited a visible oil slick on the seawater surface.
Aquaculture low	Seawater sampled from the surface water (approximately 0.5-1 m depth) about 2 km away from an aquaculture farm in the West Coast of Norway in April 2017. We presume that this sample was collected from an unpolluted site.
Aquaculture high	Seawater sampled from the surface water (approximately 0.5-1 m depth) close to an aquaculture farm in the West Coast of Norway in April 2017.
Pristine 1	Seawater sampled from the surface water (approximately 0.5-1 m depth) between Kvitsøy and Mosterøy (Norway) in August 2015. We presume that this sample was collected from an unpolluted site.
Pristine 2	Seawater was pumped from 75 m depth from the fjord outside the IRIS facility (Mekjarvik, Norway) and was sand filtered to remove gross particles. This sample is expected to be unpolluted and was collected in April 2017.

### 3.2.2 Samples collected through different experimental set ups for marker testing and selection

Purpose-designed laboratory exposures were performed to obtain 'positive controls' for hydrocarbon contaminated seawater, seawater exhibiting high nutrient loads. The experimental set ups are presented in Table 3.2.

Table 3.2: Descriptions of laboratory exposures

Name of sample	Description
Oil 2000 ppb_11d	This sample is from a previous lab exposure experiment performed at IRIS in June 2015. Seawater was pumped from 75 m depth from the fjord outside the IRIS facility (Mekjarvik, Norway) and was sand filtered before use. The seawater was poured into an exposure tank before 2000 ppb (v/v) of oil was added. The exposure tank was then left for incubation at 4°C for 11 days. This sample is expected to be a positive control for the qPCR assays related to hydrocarbon degradation.
Exposure control	5 l of sand filtered seawater collected from 75 m depth outside the IRIS facility was incubated in room temperature for 3 days in June 2017.
Exposure crude oil	5 l of sand filtered seawater collected from 75 m depth outside the IRIS facility was added 5 ml of oil and was incubated in room temperature for 3 days in June 2017.





Exposure nutrients	5 l of sand filtered seawater collected from 75 m depth outside the IRIS facility was added 5 g of sucrose and was incubated in room temperature for 3 days in June 2017.
Exposure Crude oil+nutrients	5 l of sand filtered seawater collected from 75 m depth outside the IRIS facility was added 5 g of sucrose + 5 ml oil and was incubated in room temperature for 3 days in June 2017.

### 3.2.3 Cruise sample collection in conjunction with WP4 JRAP3

Through WP4 JRAP3 on chemical contamination, an intensive sampling campaign was conducted on board the Color Fantasy “FerryBox” cruise vessel between Oslo and Kiel, between the 24 and 26 January 2017. Sixty seawater samples were collected at regular intervals during the cruise and analysed for a wide range of chemical contaminants originating from a multitude of sources. These included: a range of insecticides and herbicides from agricultural run-off; a range of pharmaceuticals, personal care products and artificial food additives emitted from urban and zoo-technical wastewater effluents; and a range of polycyclic aromatic hydrocarbons (PAHs) as markers of oil pollutions and combustion related sources. In parallel to this, 1L triplicate seawater samples were vacuum-filtered onto 0.22- $\mu$ m pore size nitrocellulose filters (Millipore) and stored at - 80°C in 2 ml Eppendorf tubes until further processing. All assays for the quantification of microbial marker species and genes developed through WP3 activities will be performed on these samples and analysed to both validate the markers through this field campaign for WP3 and to investigate the correlations between chemical, physical and biological data for WP4.

## 3.3 Preliminary results on assays and marker robustness

1L seawater samples from environmental sources or from laboratory exposures were vacuum-filtered through 0.22  $\mu$ m pore size nitrocellulose Millipore filters, then immediately stored at - 80°C in 2 ml Eppendorf tubes until DNA and RNA extractions. Primers were designed for the quantification of the different species and genes through real-time Polymerase Chain Reaction (rt-qPCR) using TaqMan probes (Nadkari et al, 2002) or CYBR green (Kwok et al, 2014), depending on the assay. The efficiency of the different assays was evaluated through standard curves and melting curves, and testing of the different primer sets on pristine seawater samples, as well as purpose sampled contaminated environmental or laboratory samples.

### 3.3.1 Total number of bacteria assay

Figure 3.1 shows the qPCR results for the quantification of total number of bacteria in selected seawater samples.



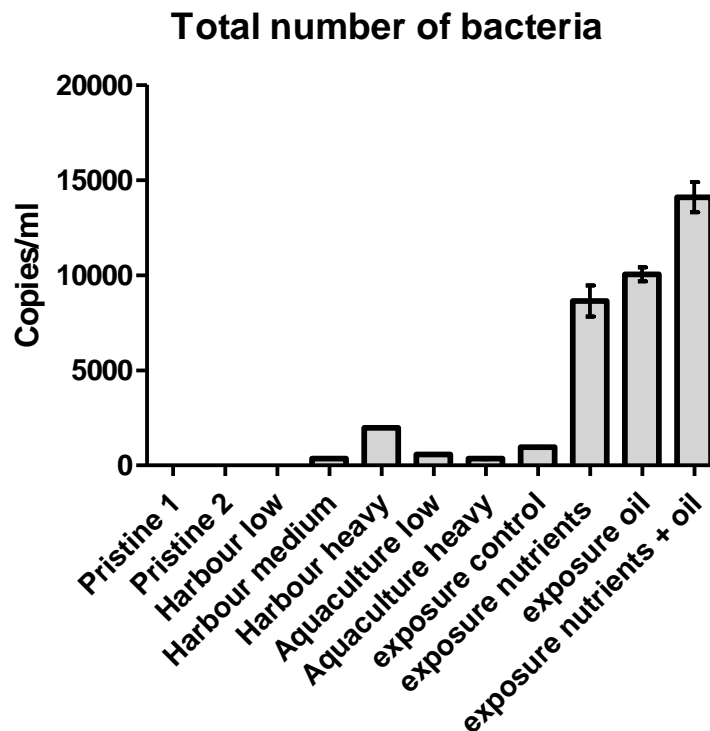


Figure 3.1: Total number of bacteria in various sea water samples in gene copy number, quantified by real-time PCR (qPCR). Sampling location and pollution load and/or treatment is indicated in the sample name.

Based on the efficiency and the melting curve analysis of the assay (data not shown), it was concluded that the assay meets the standards for selection (efficiency >80%, 1 peak). The total bacteria counts show a low number of organisms in pristine seawater areas and areas of very low contamination (pristine 1 and 2, Harbor low, Aquaculture low), and a significantly higher number of organisms in contaminated environment high in nutrient load or organic contaminants. In the environmental samples, the highest number of bacteria was found in the harbor sample with the highest content of visible contamination (thin visible oil layer). As expected, laboratory exposures contain higher nutrient loads and ambient temperature, resulting in higher microbial numbers, in particular following oil or nutrient exposures. These preliminary results suggest that quantification of total bacterial numbers may contribute to a better understanding of the effect of pollution and nutrient availability in the marine environment.

### 3.3.2 Assay for total number of *Colwellia* organisms

Figure 3.2 shows the qPCR results for the quantification of bacteria from the *Colwellia* genus in selected seawater samples.

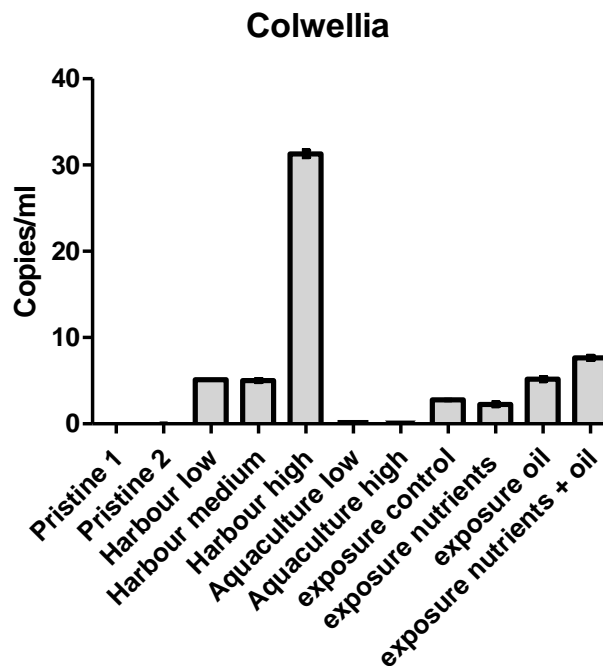


Figure 3.2: Number of *Colwellia* in various sea water samples in gene copy number, quantified by real-time PCR (qPCR). Sampling location and pollution load and/or treatment is indicated in the sample name.

Based on the efficiency and the melting curve analysis of the assay (data not shown), it was concluded that the *Colwellia* assay meets an acceptable standard for the selection criteria (efficiency >80%, 1 peak). The analysis of the control samples shows an increase of *Colwellia* numbers in the presence of oil, which may make this assay useful in detecting and monitoring hydrocarbons in the marine environment. In addition, the highest level of this organism is detectable in the harbor sample which was the most heavily contaminated with oil.

### 3.3.3 Assay for the quantification of *Oleispira antarctica* organisms

The efficiency of the *Oleispira antarctica* assay and the melting curve analysis both meets the selected criteria for acceptance (efficiency >80% and 1 peak). Figure 3.3 shows the qPCR results for the quantification of bacteria from the *Oleispira antarctica* species, from the *Oleispira* genus, in positive environmental or laboratory contaminated seawater samples, as well as in pristine environment seawater samples.

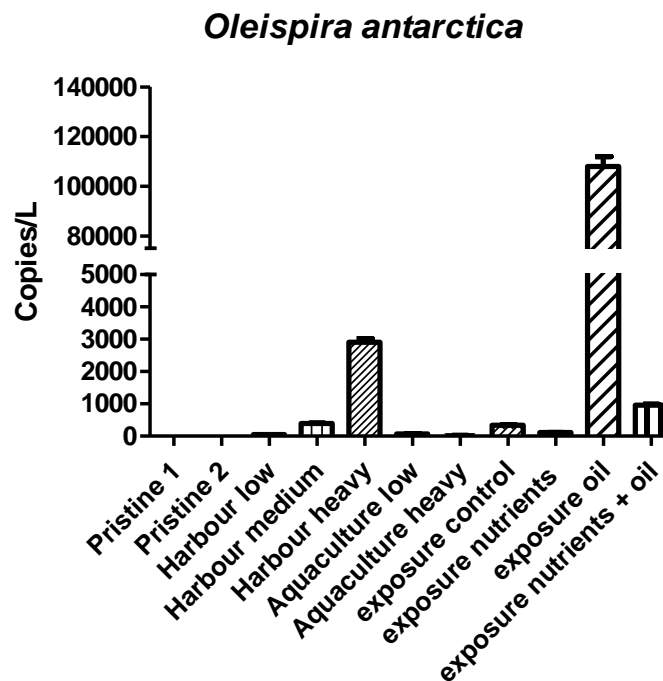


Figure 3.3: Total number of *Oleispira antarctica* in various sea water samples, in gene copy number, quantified by real-time PCR (qPCR). Sampling location and pollution load and/or treatment is indicated in the sample name.

The analysis shows an increase of *Oleispira* in the presence of oil only, and the abundance of this species in seawater depends on the level of contamination. The highest levels of this organism are found in the highly oil contaminated positive control samples as well as in the harbor sample with the visible oil contamination, suggesting this assay may be useful in monitoring hydrocarbon contaminants in the marine environment. Seawater high in other nutrient loads seem, however, to generate high number of other organisms in favor to *Oleispira*.

#### 3.3.4 Assay for the quantification of *Alteromonas*, *Marinobacter*, *Alcanivorax* (AMA) organisms

The efficiency of the AMA assay and the melting curve analysis both met the criteria for selection (efficiency >80% and 1 peak). The results from testing the assay on positive controls (environmental or laboratory contaminated samples), as well as on pristine environment seawater samples are shown in Fig 3.4.

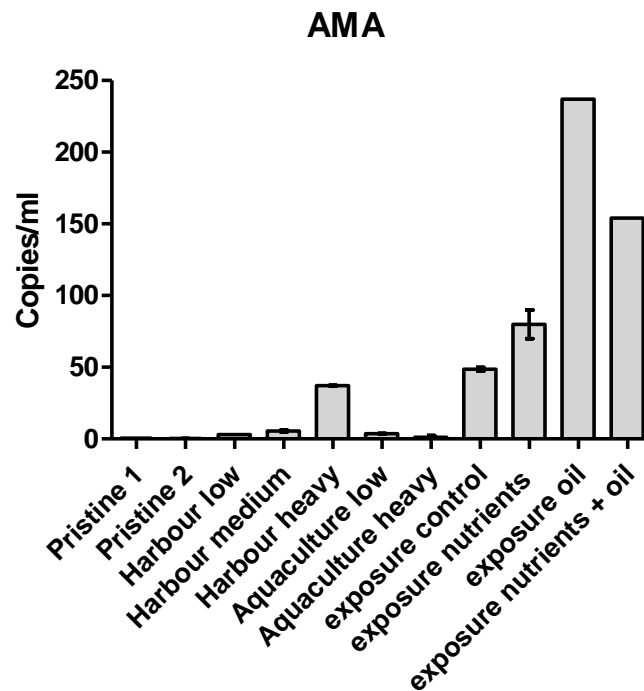


Figure 3.4: Number of AMA organisms in sea water samples, quantified by qPCR. Sampling location and pollution load and/or treatment is indicated in the sample name.

The analysis shows an increase of *AMA* in the presence of oil and that the abundance of these genera in seawater depends on the level of contamination. The highest levels of these organisms are found in the highly oil contaminated positive control samples, as well as in the harbor sample with the visible oil contamination, suggesting this assay may be useful in monitoring hydrocarbon contaminants in the marine environment.

### 3.4 Preliminary conclusions from assays

The preliminary results from this study suggest that assays for total number of bacteria and quantification of organisms from the *Colwellia*, *Oleispira*, *Alteromonas*, *Marinobacter* and *Alcanivorax* genera could be useful as indicators of hydrocarbon contaminations in the marine environment.



## 4 Metabarcoding - a tool for investigating plankton diversity and harmful algal blooms

### 4.1 Introduction to metabarcoding of plankton

Metabarcoding is a relatively new tool for investigating plankton. The following methods are other approaches for investigating phytoplankton biodiversity and biomass (see JRAP#1):

1. Methods based on the morphology of organisms:
  - a. Microscopy – hundreds of cells are identified and sized by a skilled microscopist with expertise in identifying phytoplankton.
  - b. Imaging in flow methods, e.g. Imaging Flow Cytometry (see JRAP#1), typically tens of thousands of cells are counted and imaged individually. Automated image analysis is used for processing images.
2. Methods based on pigment composition in organisms:
  - a. Methods based on measuring photosynthetic pigments of microalgae, e.g. by measuring the fluorescence or absorption of pigments using single or multi spectral instruments. Bulk properties of a mixture of plankton organisms are measured.
  - b. Methods based on investigating fluorescence and scattering properties of individual cells - Flow cytometry. Typically tens of thousands of cells are counted and characterized.
  - c. Methods based on analysing photosynthetic pigments in water samples concentrated by filtration. Pigments are extracted using solvent, such as ethanol, methanol or acetone, and analysed using a fluorometer or spectrophotometer. Traditionally Chlorophyll. a is used as a proxy for phytoplankton biomass. Separating pigments using High Performance Liquid Chromatography (HPLC) makes it possible to also differentiate algal groups based on pigment composition.

When doing metabarcoding, phytoplankton are concentrated from water samples, usually by filtration. Most often, 16S and 18S rDNA are sequenced since these genes have the enough variability to make it possible to differentiate different plankton. 16S is used for prokaryotic organisms, e.g. cyanobacteria, and also for chloroplasts, while 18S is used for eukaryotic organisms. 454 pyrosequencing used e.g. by Egge et al. (2013) have recently been replaced with high throughput sequencing, (e.g. Hu et al. 2016; de Vargas et al. 2015). This is described in some more detail below.

In this subtask, the focus is to evaluate rDNA metabarcoding as a tool for studying the biodiversity of plankton with a focus on harmful algae. This includes working with data from samples already collected during the JERICO-project and with samples from a harmful algal bloom (HAB) study near a mussel farm at Tångesund, Sweden, carried out Aug. to Oct. 2016. The HAB study is part of WP3.1 and WP4.1 (JRAP#1). The multi-method study at Tångesund gives valuable reference data for the metabarcoding work carried out there. A direct comparison between metabarcoding, *in situ* imaging flow cytometry and microscopy will be possible.



## 4.2 Preliminary results

### 4.2.1 Ferrybox samples



Fig. 4.1. The merchant vessel *TransPaper* carries cargo on the route Lübeck- Kemi-Olou- Lübeck every week. SMHI and SYKE operate a Ferrybox system on the ship. The Ferrybox system includes a pump, sensors for conductivity, temperature, oxygen, chlorophyll fluorescence, phycocyanin fluorescence and CDOM-fluorescence. Water samples for rDNA barcoding were collected from the debubbler shown in the left part of the image. Water inlet is at approximately 3 m depth.

The Ferrybox system on the merchant vessel *TransPaper* (Fig. 4.1) was used to collect samples during the JERICO-project in summer 2013. The Ferrybox system is described by Karlson et al. (2016). Sampling locations are illustrated in Fig. 4.2. Sampling was manual and samples were filtered directly after collection and frozen in liquid nitrogen on the ship. Microscopy was used for traditional description of the plankton community based on the morphology of the organisms. 16S and 18S rDNA was analysed for metabarcoding. The metabarcoding results are published (Hu et al. 2016). Here follows a summary of the results based on both microscopy and metabarcoding.

The sampling covers a large salinity range from around 3 to 25 psu (Fig. 4.3). Biomass estimated as chlorophyll was low, in the range of 0-3  $\mu\text{g L}^{-1}$ . Temperature range was approximately 13-19°C. In total, approximately 1800 unique taxonomical units (OTU) from unicellular eukaryotic organisms and cyanobacteria were detected in 18 samples. Microscopy yielded 89 different taxa. A summary of the metabarcoding based results is presented in Figs. 4.4 and 4.5. Microscopy based cell numbers, biovolumes and biomass in carbon units are presented in Fig. 4.6.

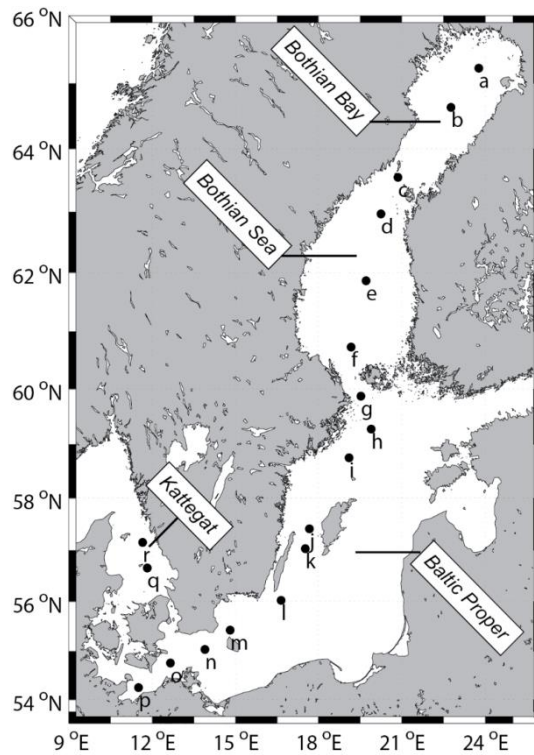


Fig. 4.2. Locations for collecting samples for rDNA metabarcoding and microscopic analys of phytoplankton collected during the JERICO-project in July 2013.

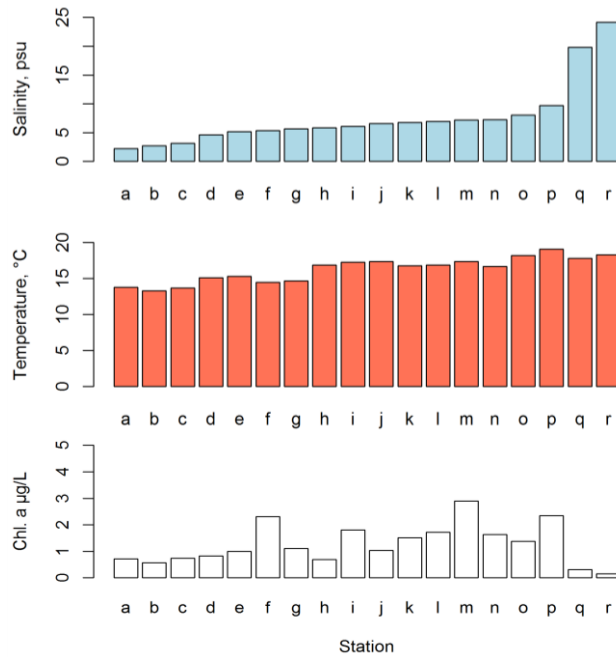


Fig. 4.3 Top to bottom: Salinity, temperature and concentration of chlorophyll a at the different sampling sites.





Table 4.1. List of organisms noted in samples analysed using microscopy from 18 stations. In total, 89 different taxa were observed using microscopy.

Plankton Group	Class	Scientific name	Trophic type
Ciliophora	Gymnostomatea	Mesodinium rubrum	MX
Ciliophora	Oligotrichea	Helicostomella subulata	HT
Ciliophora	Prostomatea	Tiarina	HT
Ciliophora	Unidentified ciliates	Ciliophora	HT
Cryptophyta	Cryptophyceae	Hemiselmis	AU
Cryptophyta	Cryptophyceae	Leucocryptos marina	HT
Cryptophyta	Cryptophyceae	Plagioselmis prolonga	AU
Cryptophyta	Cryptophyceae	Teleaulax	AU
Cyanobacteria	Cyanophyceae	Anabaena	AU
Cyanobacteria	Cyanophyceae	Aphanizomenon	AU
Cyanobacteria	Cyanophyceae	Aphanizomenon flos-aquae	AU
Cyanobacteria	Cyanophyceae	Aphanocapsa	AU
Cyanobacteria	Cyanophyceae	Aphanothece paralleliformis	AU
Cyanobacteria	Cyanophyceae	Cyanodictyon	AU
Cyanobacteria	Cyanophyceae	Lemmermanniella	AU
Cyanobacteria	Cyanophyceae	Nodularia spumigena	AU
Cyanobacteria	Cyanophyceae	Pseudanabaena limnetica	AU
Cyanobacteria	Cyanophyceae	Snowella	AU
Cyanobacteria	Cyanophyceae	Woronichinia	AU
Bacillariophyta	Bacillariophyceae	Bacillariophyceae	AU
Bacillariophyta	Bacillariophyceae	Cylindrotheca closterium	AU
Bacillariophyta	Bacillariophyceae	Diatoma tenuis	AU
Bacillariophyta	Bacillariophyceae	Nitzschia paleacea	AU
Bacillariophyta	Bacillariophyceae	Pseudo-nitzschia	AU
Bacillariophyta	Coscinodiscophyceae	Actinocyclus	AU
Bacillariophyta	Coscinodiscophyceae	Dactyliosolen fragilissimus	AU
Bacillariophyta	Coscinodiscophyceae	Guinardia delicatula	AU
Bacillariophyta	Coscinodiscophyceae	Guinardia flaccida	AU
Bacillariophyta	Coscinodiscophyceae	Leptocylindrus danicus	AU
Bacillariophyta	Coscinodiscophyceae	Leptocylindrus minimus	AU
Bacillariophyta	Coscinodiscophyceae	Proboscia alata	AU
Bacillariophyta	Coscinodiscophyceae	Thalassiosira levanderi	AU
Bacillariophyta	Mediophyceae	Attheya septentrionalis	AU
Bacillariophyta	Mediophyceae	Chaetoceros	AU
Bacillariophyta	Mediophyceae	Chaetoceros affinis	AU
		Chaetoceros ceratosporus var.	
Bacillariophyta	Mediophyceae	ceratosporus	AU
Bacillariophyta	Mediophyceae	Chaetoceros crinitus	AU
Bacillariophyta	Mediophyceae	Chaetoceros danicus	AU
Bacillariophyta	Mediophyceae	Chaetoceros impressus	AU
Bacillariophyta	Mediophyceae	Chaetoceros pseudobrevis	AU
Bacillariophyta	Mediophyceae	Chaetoceros subtilis var. subtilis	AU
Bacillariophyta	Mediophyceae	Chaetoceros thronsdensii var. thronsdensii	AU



Bacillariophyta	Mediophyceae	Chaetoceros wighamii	AU
Dinophyta	Dinophyceae	Alexandrium ostenfeldii	AU
Dinophyta	Dinophyceae	Amphidinium sphenoides	HT
Dinophyta	Dinophyceae	Ceratium fusus	AU
Dinophyta	Dinophyceae	Ceratium longipes	AU
Dinophyta	Dinophyceae	Ceratium tripos	AU
Dinophyta	Dinophyceae	Cladopyxis claytonii	AU
Dinophyta	Dinophyceae	Dinophysis acuminata	MX
Dinophyta	Dinophyceae	Dinophysis norvegica	MX
Dinophyta	Dinophyceae	Gymnodiniales	HT
Dinophyta	Dinophyceae	Gymnodinium	HT
Dinophyta	Dinophyceae	Gymnodinium simplex	AU
Dinophyta	Dinophyceae	Heterocapsa rotundata	AU
Dinophyta	Dinophyceae	Heterocapsa triquetra	MX
Dinophyta	Dinophyceae	Katodinium glaucum	HT
Dinophyta	Dinophyceae	Oblea rotunda	HT
Dinophyta	Dinophyceae	Phalacroma rotundatum	HT
Dinophyta	Dinophyceae	Prorocentrum cordatum	AU
Dinophyta	Dinophyceae	Protoperidinium	HT
Dinophyta	Dinophyceae	Protoperidinium brevipes	HT
Dinophyta	Dinophyceae	Protoperidinium steinii	HT
Dinophyta	Dinophyceae	Pyrophacus horologium	AU
Dinophyta	Dinophyceae	Scrippsiella	AU
Dinophyta	Dinophyceae	Scrippsiella hangoei	AU
Euglenozoa	Euglenophyceae	Eutreptiella	AU
Chlorophyta	Chlorophyceae	Desmodesmus armatus var. armatus	AU
Chlorophyta	Chlorophyceae	Eudorina elegans	AU
Chlorophyta	Chlorophyceae	Monoraphidium contortum	AU
Chlorophyta	Chlorophyceae	Monoraphidium griffithii	AU
Chlorophyta	Chlorophyceae	Monoraphidium minutum	AU
Chlorophyta	Prasinophyceae	Pyramimonas	AU
Chlorophyta	Prasinophyceae	Pyramimonas virginica	AU
Chlorophyta	Trebouxiophyceae	Oocystis	AU
Chlorophyta	Ulvophyceae	Planctonema lauterbornii	AU
Haptophyta	Prymnesiophyceae	Chrysochromulina	MX
Ochrophyta	Chrysophyceae	Dinobryon	MX
Ochrophyta	Chrysophyceae	Dinobryon divergens	MX
Ochrophyta	Chrysophyceae	Dinobryon faculiferum	MX
Ochrophyta	Chrysophyceae	Paraphysomonas	HT
Others	Cryptophyta, ordines incertae sedis	Katablepharis	HT
Ochrophyta	Dictyochophyceae	Dictyocha speculum	AU
Others	Ebriophyceae	Ebria tripartita	HT
Charophyta	Klebsormidiophyceae	Elakatothrix gelatinosa	AU
Unidentified	Unidentified cells without flaggella	Unicell	AU
Unidentified	Unidentified flagellates, autotrophic	Flagellates	AU
Unidentified	Unidentified flagellates, heterotrophic	Flagellates	HT





Table 4.2. A list of the major groups of organisms identified using metabarcoding of 16S and 18S rDNA in 18 samples.

Main taxonomic group (according to SILVA- and PR2-databases)	Examples of marine organisms in the group	Number of unique OTU
Bacteria	Bacteria, including cyanobacteria and chloroplasts	1243
Cyanobacteria	Cyanobacteria	36
Alveolata	Dinoflagellates, ciliates	415
Apusozoa	flagellate organisms	1
Archaeplastida	Green algae, red algae	107
Hacrobia	Cryptophyta and Haptophyta	132
Opisthokonta	Metazoa, choanoflagellates and choanoflagellates	90
Stramenopiles	Diatoms, etc.	278
Rhizaria	Foraminifera, radiolaria etc.	169
Eukaryotic organism from other groups		563
<i>Total number of unicellular eukaryots</i>		1755



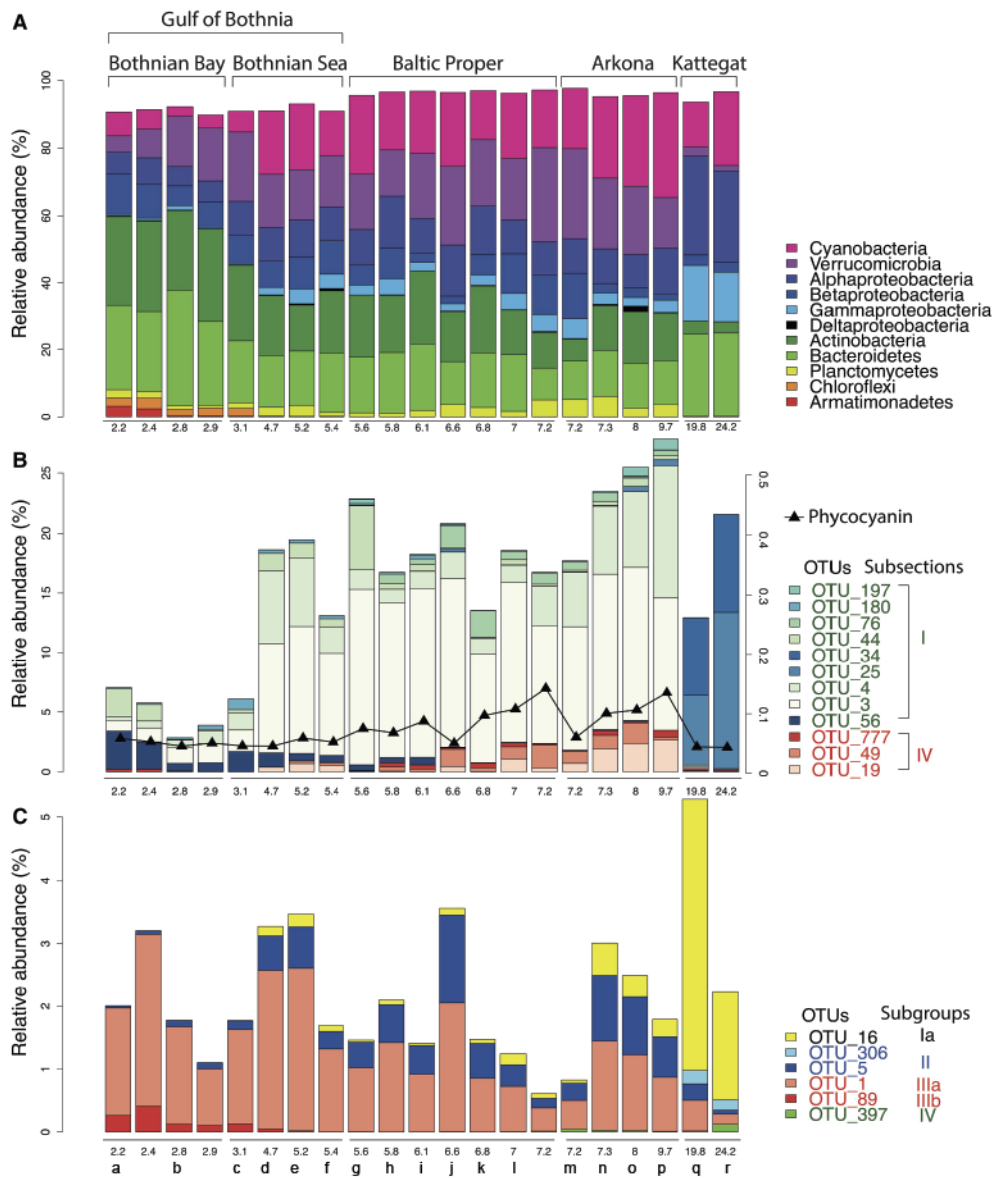


Fig. 4.4. Relative abundance of cyanobacteria based on metabarcoding of 16S rDNA. X-axes show both station name and salinity. A shows the major groups of bacteria, B shows dominant cyanobacteria-OTU:s (Subsection I include pikocyanobacteria), OTU\_56 is a *Microcystis*. Subsection IV contain filamentous cyanobacteria, OTU\_777, OTU\_49 and OTU\_19 belong to *Aphanizomenon*, *Nodularia* and *Dolichospermum* (syn. *Anabaena*). C shows the bacteria group SAR11. Modified after Hu et al. 2016.

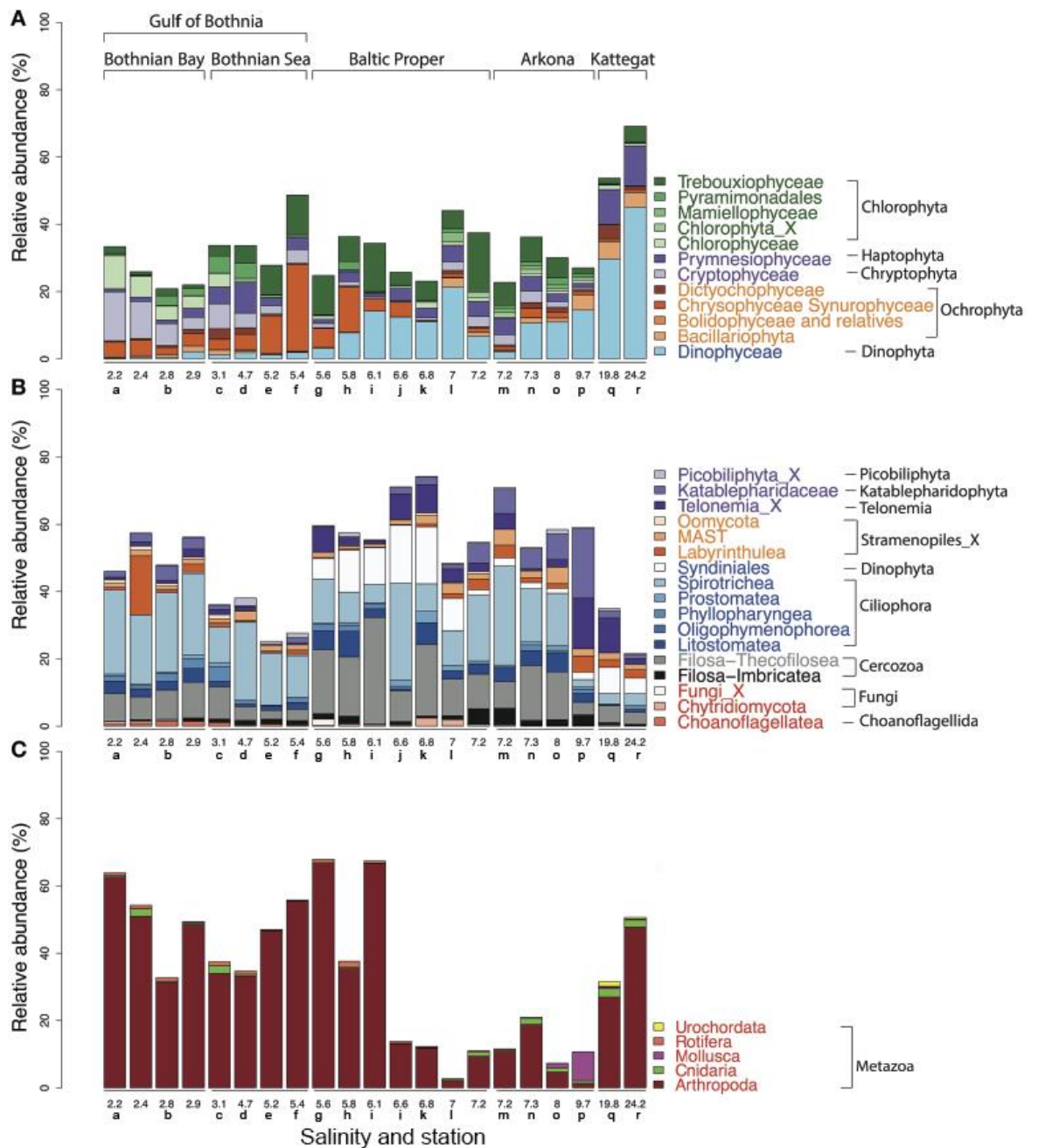


Fig. 4.5. Relative abundance of eukaryotic organisms identified using meta-barcoding. X-axes show both salinity and station name. A shows relative abundance of different classes of mainly auto- and mixotrophic groups of eukaryotic plankton. B shows relative abundance of mainly heterotrophic groups of plankton. C shows relative abundance of metazoa. Modified after Hu et al. 2016.

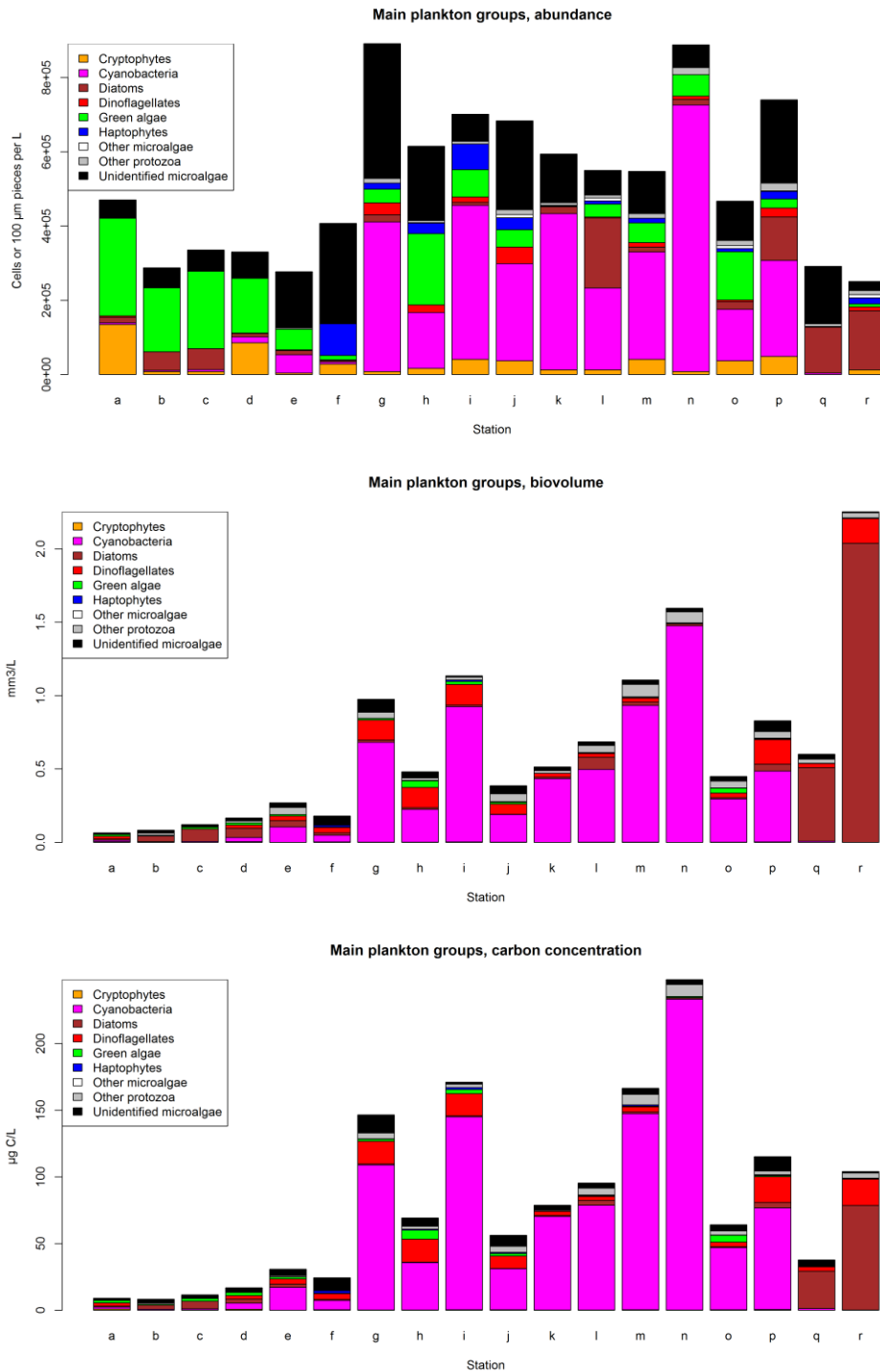


Fig. 4.6 Microscopy-based data showing the main groups of unicellular organisms. Top: Cell numbers, middle: biovolume, bottom: biomass in carbon units.



#### 4.2.1 About preservation of samples for rDNA analyses of plankton

Preserving plankton samples for later rDNA analysis is problematic. Several different preservatives have been tested and will be discussed during the Symposium: *High throughput methods for application in marine biodiversity time series: Addressing their challenges to fulfil their promises*, 11-13 October 2017.

In the data set from TransPaper collected in 2013, Lugols iodine was tested. The number of OTU:s detected were much lower when samples were preserved with Lugols iodine compared to direct filtering and freezing in liquid nitrogen.

#### 4.2.2 A harmful algal bloom study at Tångesund, Swedish west coast

In August to October 2016, an intense study of harmful algae and phytoplankton diversity in general was carried out next to a mussel farm on the west coast of Sweden. The study was multidisciplinary including physical oceanography and *in situ* imaging flow cytometry, as well as weekly water sampling for microscopic analysis of plankton, nutrients and chlorophyll. Water samples for metabarcoding analysis of plankton were also collected. Samples are being analysed at Alfred Wegener Institute in Germany and at the Science for Life Laboratory in Stockholm, Sweden.





## 5 Biosensors for the detection of toxic algae

This task aims at developing complementary technologies for monitoring toxic algae based on the detection of the organisms through an autonomous sensor, and the detection of the toxin using a probe. Within the EU project EnviGuard (Project no. 614057), a fully automated sensor module for autonomous monitoring of toxic algae will be developed by the Alfred Wegner Institute (AWI), Germany, in cooperation with HZG. This system includes a remote-controlled automated filtration system coupled to a semi-automated nucleic acid biosensor. The detection principle of the nucleic acid biosensor is based on the specific binding of a molecular probe immobilised to the sensor surface to the target particle. A transducer component transforms this detection event into a measurable signal, such as an electrical current for highly sensitive and quantitative nucleic acid based detection of toxic algae. In this activity, this sensor will be adapted and optimised for long term unattended operation on the Ferrybox systems. In parallel, a complementary technology for the detection of the toxins will be further developed. An *in situ* optical biosensor based on surface plasmon resonance for domoic acid detection and quantification has been developed at Ifremer. Tests performed in the laboratory, and during oceanographic campaigns, showed that the system allows a semi-quantitative detection of the toxin in the range 0,1-2 ng/mL. Improvements will be made through this task to gain in sensitivity, accompanied with a drastic reduction in costs, by working in the NIR range with special glass material and low-cost spectrometer. This strategy will allow a rapid adaptation of the *in situ* prototype and testing in the marine environment in the context of "JERICO-NEXT". The system will be complementary to the one developed by the HZG. Analysis of the same samples with the two instruments will be carried out to prove the interest to detect the algae species, as well as the toxin, in coastal waters.

### 5.1 Detection of toxic algae through nucleic acid detection

The aim of Task 4.1 is the adaptation and application of an automated molecular based biosensor for the detection of microalgae for regular monitoring of potentially toxic algal species, to be operated on FerryBox systems. Such an autonomous quantitative nucleic acid based detection sensor for microalgae species, mainly dinoflagellates, which have the potential to form Harmful Algal Blooms, is under development in the EU project EnviGuard. The instrument consists of an automated filtration device for marine microorganisms (AUTOFIM), including re-suspension of the particulate organic matter on the filter by application of a lysis buffer solution and subsequent analysis with a rRNA biosensor by electrochemically detection on a chip with molecular probes. The filtration system AUTOFIM is designed for autonomous filtration of water samples up to five liters. In total, 12 different samples can be taken. The measured current from the biosensor chip can be used as a quantitative signal of cell amounts. The algae detection unit is calibrated for certain algal species which are typically for the North Sea. One of them are Dinophysis, which are one of the main threat to aquaculture in Europe. The single components of this system have been developed and tested. Fig 5.1 shows the algae detection unit.



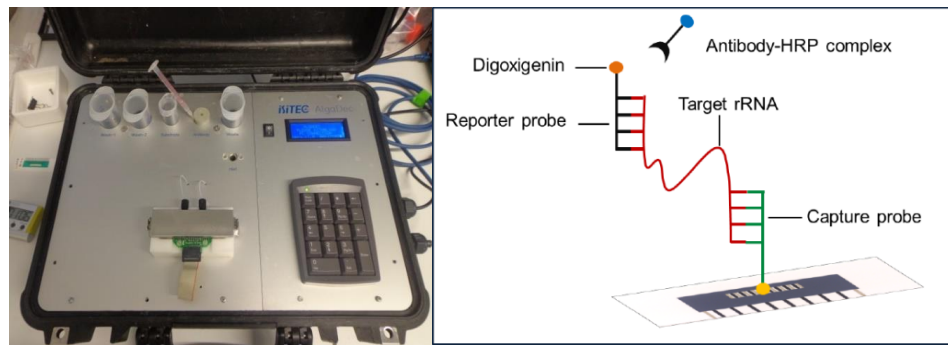


Figure 5.1 Algae detection unit (Foto Metfies, AWI)

In the EnviGuard project, the assembly of the automated sampler AUTOFIM and the algae sensor has been successfully tested on a cruise with the research vessel Polarstern (Metfies et al., 2016). Currently, the biosensor is calibrated for *Alexandrium minutum*, *Alexandrium tamarense/fundyense*, *Protoceratium reticulum*, *Dinophysis acuminata/acuta* and *Pseudonitzschia* sp.

A typical correlation between signal intensity of the bio-sensor and the cell abundance is shown in Fig 5.2.

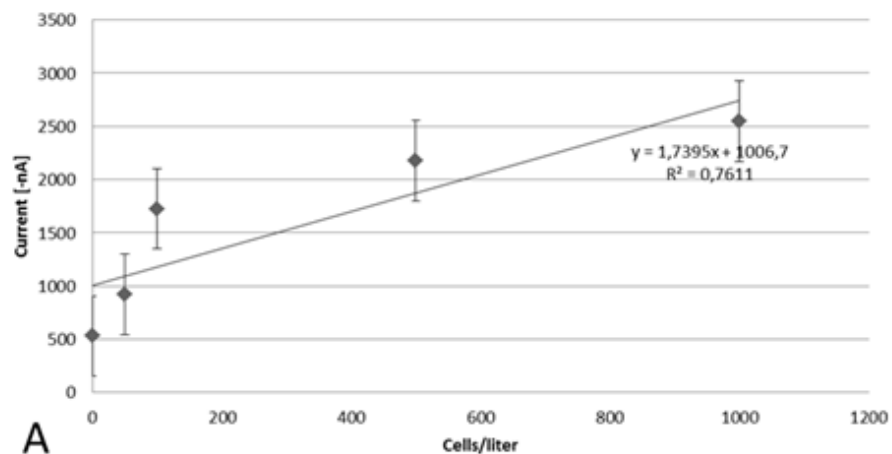


Figure 5.2 Correlation between signal intensity (current) and cell amounts for *Dinophysis* sp. (from Metfies et al., EnviGuard)

In spring 2017, the complete system has been optimized for automated operation and a first deployment and field test started on the island Helgoland, next to a stationary FerryBox for half a year. Figure 5.3 shows the complete setup of autosampler, filtration unit and biosensor.



Fig. 5.3: Filtration, sample preparation and detection unit under development in the EU project EnviGuard. (Foto AWI)

Within JERICO-NEXT, a next step will be to operate this biosensor in connection with an underway FerryBox which requires a stable and autonomous behavior of the complete assembly. The development and final test of this complex device is delayed in the EnviGuard project and will be not completed until beginning of 2018. Due to this delay, the device will be available at the earliest beginning of 2018. Thus, currently no JERICO-NEXT specific work in this task could be carried out.

## 5.2 Development of an in-situ optical sensor for the detection of toxins

For the last decades, Surface Plasmon Resonance (SPR) sensors have spread over many areas (Homola, 2006). SPR is an optical phenomenon that can be exploited to measure the changes of refractive index as small as  $10^{-7}$  at the close vicinity of a surface. Such a high sensitivity is even capable of detecting few  $\text{pg}/\text{mm}^2$  of molecules that get adsorbed on the surface. SPR sensors are therefore often presented as optical scales.

They can be turned into a specific sensor thanks to the surface functionalization. If a layer specific to a molecule is deposited on the surface, only the target compound can reach the surface.

SPR sensors are sensitive to the amounts of molecules on the surface. They are thus quantitative and very versatile. As far as a specific layer can be synthesized; any kind of molecules or micro-organisms can be detected specifically: methane (Boulart et al., 2008), carbon dioxide (Lang et al., 2012), metallic ions (Wu et al., 2004; Ock et al., 2001), pesticides (Minunni et al., 1993; Harris et al., 1999), polycyclic aromatic hydrocarbon (Gobi et al., 2004), and phycotoxin (Iotierzo et al., 2004; Yu et al., 2005; Campell et al., 2011; McNamee et al., 2013).



However, few SPR sensors are used in operational oceanography although the tremendous need for specific, sensitive and quantitative monitoring tools. To our knowledge, only three *in situ* SPR systems have been reported: two of them as refractometer (Diaz-Herrera et al., 2006; Kim et al., 2011) and one as biosensor of Domoic Acid (DA) (Colas et al., 2016); a phycotoxin responsible for Amnesic Shellfish Poisoning (ASP).

The latter was developed by Ifremer. It was demonstrated capable of detecting DA in operational conditions at concentration as low as 0.1 ng/mL. The sensor could be used about 10 times and the SPR sensor was regenerated by the injection of a low concentration NaOH solution.

This work demonstrated the strong potential of SPR sensors for oceanography. However, it suffered from few limitations. First, only one measurement channel was available. This means that only one kind of molecule can be assayed. Second, the dynamic range was relatively small (0.1 to 2 ng/mL). Third, the reference channel could not compensate the signal drift, resulting in a poor reproducibility and an error measurement of 0.3 ng/mL. Last, the system was made of some expensive optical components that limited its cost efficiency. In the context of the JERICO-NEXT project, a novel sensor with innovative design is being developed to address these issues.

The new system is based on SPR imaging (SPRi). This technology takes an image of the SPR sensor surface (also called the SPR chip), which has been functionalized by an array of specific receptors. The spots can be made of different receptors. The sensor can then detect and assay different molecules at the same time. The spots can be composed of the same receptor but at different surface concentrations. In this way, the sensor dynamic range can be extended. The spots can be specific to a reference molecule. A reference measurement can then be performed at each assay, which alleviates the issue of signal drift. The spots can also be similar. Replica measurements are then carried out at each assay and the assay accuracy can be improved. In addition, the SPR imaging apparatus requires only a camera, which makes it cost efficient. As a result, this is not an expensive technology.

The aim of this subtask is to develop an underwater SPRi system that can address the main limitations of the previous system.

This part of the report will be composed of three sub-parts. First the principle of SPRi system will be explained. Second, the design of the new system will be presented. Finally, our work about improving the chemistry will be shown, before concluding and introducing the prospects of this development.

### 5.2.1 SPRi sensors:

Surface Plasmon Resonance (SPR) is a special resonance phenomenon that can take place in metals such as silver, copper, gold, and aluminium. The electron density of the conduction band oscillates in phase. SPR can be generated when light interacts with a thin film of metal of few tens of nanometre thickness deposited on top of a dielectric material, generally a prism. Gold is often the preferred material because of its chemical stability. In addition, it can be easily functionalized because it can create strong bond with -SH or -NH<sub>2</sub> moieties.



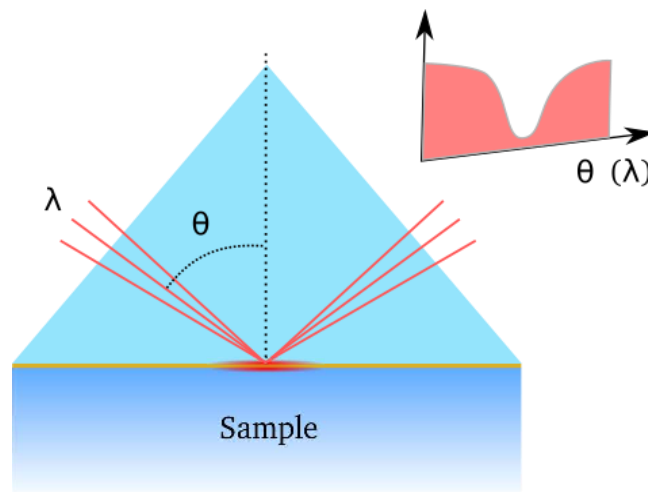


Figure 5.4: SPR sensor configuration. A thin film of noble metal is deposited on a prism. The sample is in contact with the thin film. A beam of light of angle of incidence  $\theta$  and wavelength  $\lambda$  shines the metal/prism interface. At the appropriate angle and wavelength, the light is absorbed. The reflectance presents a dip.

Let us consider a prism covered by a thin film of gold of typically 50 nm thickness. The sample circulates in the flow cell at the other side of the metallic film (Figure 5.4). A beam of light of wavelength  $\lambda$  shines the prism/metal interface at an angle of incidence  $\theta$ . It gets reflected onto the gold film and goes out of the prism. For a particular wavelength and incidence angle, noted  $\lambda_{SPR}$  and  $\theta_{SPR}$  respectively hereafter, the incoming photons interact with the conduction electrons that enter into resonance. The incoming power is then transferred to the metal. There is a minimum of reflected light power.

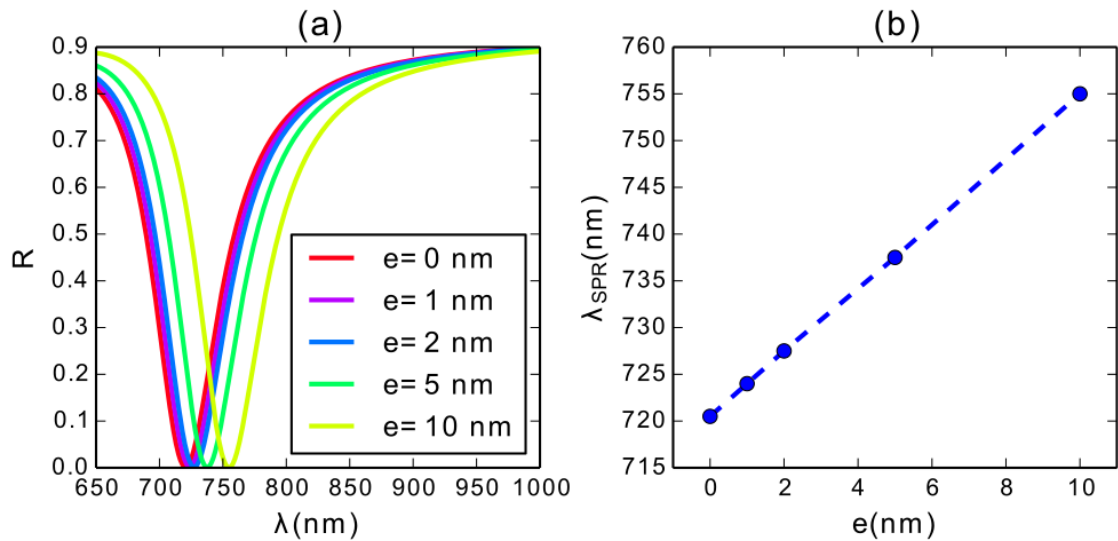


Figure 5.5: Reflectance of a collimated and polychromatic beam as a thin film of biomolecule grows on the surface from a thickness ( $e$ ) of 0 to 10 nm (a) and the corresponding resonance wavelength ( $\lambda_{SPR}$ ) with regards to  $e$  (b).

The SPR leads to an evanescent wave propagating at the interface over a distance of few microns. Its penetration depth is typically of few hundreds of nanometres. This evanescent wave probes the sample medium. Then, only the events that occur at the vicinity of the metal film (typically less than 100 nm) make the dip shift.

Let us consider the previous configuration. The surface is assumed to be functionalized with a specific receptor. The sample is injected. A molecular layer gets formed as the target molecule is captured by the surface chip. In Figure 5.5a, the reflectance with regards to the wavelength for a fixed incidence angle and five layers thickness values (noted  $e$ ) are superimposed. As  $e$  increases, the dip shifts toward higher wavelengths. In the range considered in this example, the resonance wavelength changes linearly with the molecule thickness (Figure 5.5b) and then to the amount of molecule absorbed on the surface.

A scheme of a typical SPRi apparatus is drawn in Figure 5.6. A monochromatic LED emits a beam of light, collimated by a lens. A polarizer linearly polarizes the light. The beam then gets into the prism, gets reflected on the gold thin film and goes out of the prism. A pair of lens then constitutes an afocal system that images the chip on the matrix of a camera.

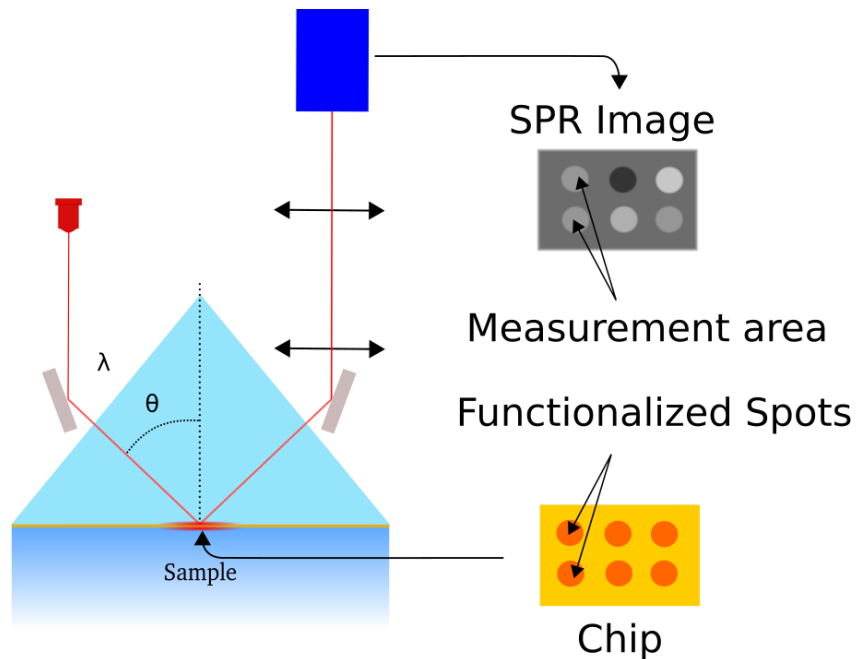


Figure 5.6: Schema of a typical SPRi system

A map of the reflectance changes over the substrate is then grabbed by the camera. If the metal layer is functionalized with different spots, each of them corresponding to a specific layer, the metal layer is turned into a real biochip. Several components can then be detected and assayed at the same time.

The development of such a system requires the optimization of the configuration and choice of the different components. The main parameters and components to choose are: the LED wavelength, the glass material of the prism, the angle of incidence on the gold thin film, the camera and the afocal system. The next part will detail all these points.

### 5.2.2 Design of the SPRi sensor:

Let S be defined as the sensitivity of the sensor to the refractive index change:

$$S = \frac{\partial R}{\partial n}$$

The value of S depends on the metal, the glass material, the thin film thickness and the wavelength, which should be optimized for a particular detection configuration.

The sensor we developed is expected to detect the smallest amount of molecule that reacts with the functionalizing layer. The optimisation process consisted in determining the small surface concentration (noted  $d\Gamma_{min}$ ) that can be detected. It can be shown that:

$$\delta\Gamma_{min} \propto \frac{\delta R_{min}}{S}$$



where  $\delta R_{min}$  is the smallest the reflectance that can be measured. It mainly depends on the signal to noise ratio of the signal at the camera.

The design of the new biosensor requires the optimisation and choice of the different parts. The next sections will detail these points.

#### **The light source:**

The sensitivity of the SPRi system depends mainly on the wavelength of the light source. It is known that the higher the wavelength, the higher the sensitivity (Maillart, 2004). However, the maximum sensitivity of standard camera is in the 500-600 nm range. Their quantum efficiency gets very low above 850 nm. The light source wavelength is then chosen between 750 and 850 nm.

The response of the SPR system depends strongly on the incidence angle ( $\theta$ ) on the gold thin film. This raised an issue for operational use. When the SPR chip is replaced,  $\theta$  might change slightly, which might have the dip gone out of the measurement range for this wavelength. In addition,  $\lambda_{SPR}$  depends on the refractive index of the sample. The dip can get out of range of the system for some samples. Thus, we decided to implement a light source made of seven LEDs whose wavelength ranges from 750 to 850 nm. Each of the LEDs is injected in an optical fibre that is connected to an optical switch (Dicon). This component is driven by an electronics board connected to a computer. Then, after replacing the SPR chip, the optimal wavelength can be chosen.

#### **The prism material and geometry:**

In the case of SPRi, high refractive index material yields to the highest sensitivity (Maillart, 2004). We compared three configurations based on three common optical glasses: F2, SF11 and LASF9. Their refractive indices at a wavelength of 800 nm are equal to 1.6084, 1.7646 and 1.8325, respectively. First, the incidence angle was calculated for these three materials to have a fixed  $\lambda_{SPR}=765$  nm when the sensor is in pure water. This resonance wavelength was chosen to lay between two emission wavelengths of two the available LEDs ( $\lambda=730, 740, 750, 760, 770, 780, 800, 810, 820, 830, 840, 850$  nm). The incidence angle that was calculated equals to 59.68, 51.88 and 49.26°, respectively.



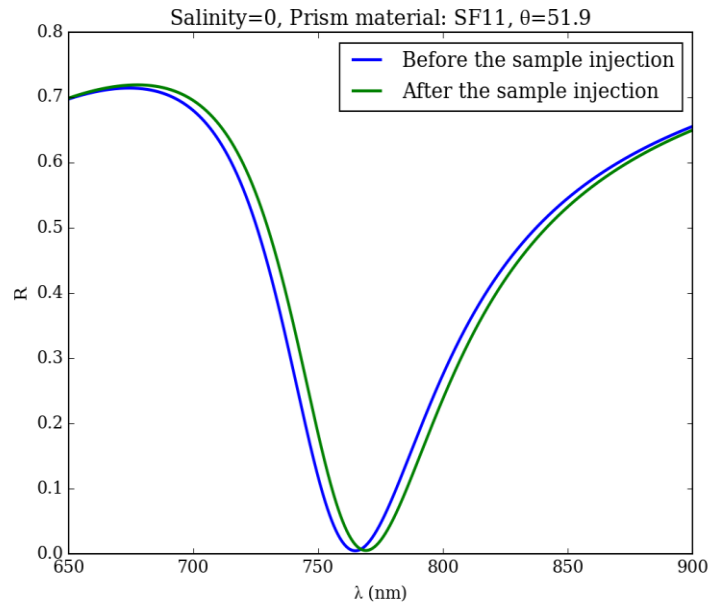


Figure 5.7: Reflectance of the SPR sensor made of SF11 before and after a 2nm film of biomolecules gets immobilized on the gold surface.

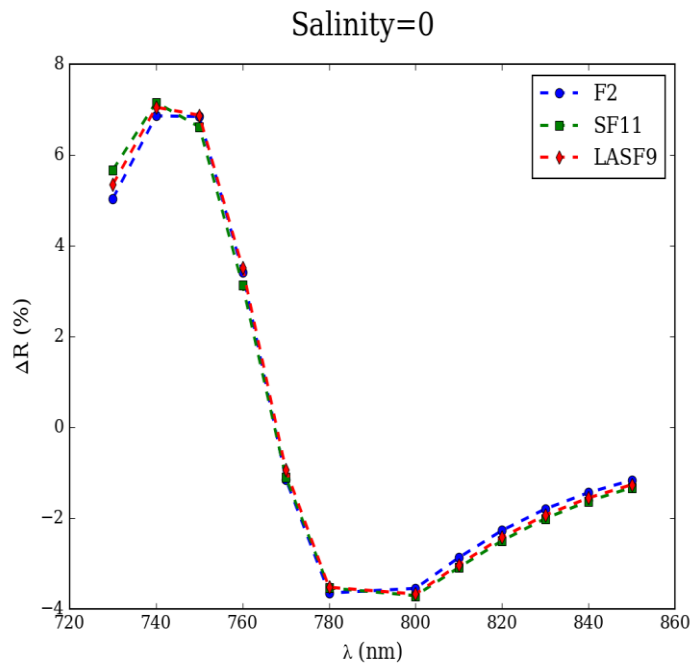


Figure 5.8: Reflectance change when the layer gets formed with regards to the illumination wavelength in the case of F2, SF11 and LASF9 prisms. The sample solvent is seawater of salinity 0.

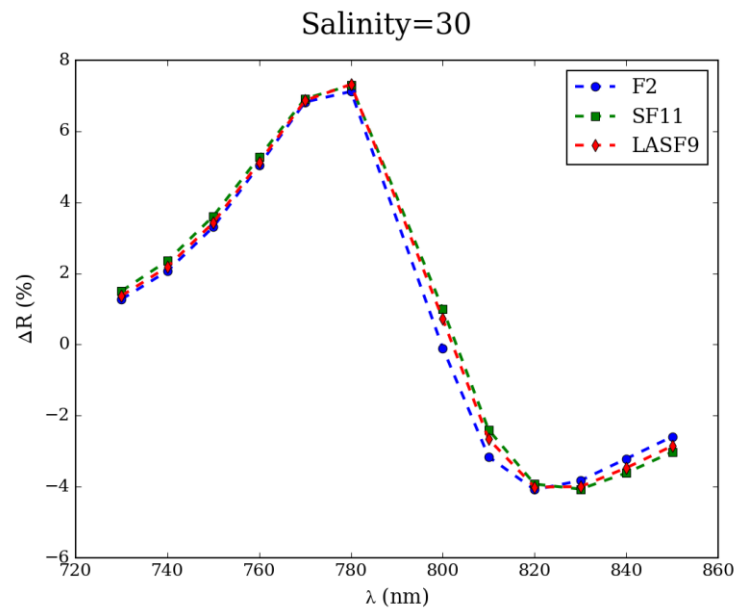


Figure 5.9: Reflectance change when the layer gets formed with regards to the illumination wavelength in the case of F2, SF11 and LASF9 prisms. The sample solvent is seawater of salinity 30.

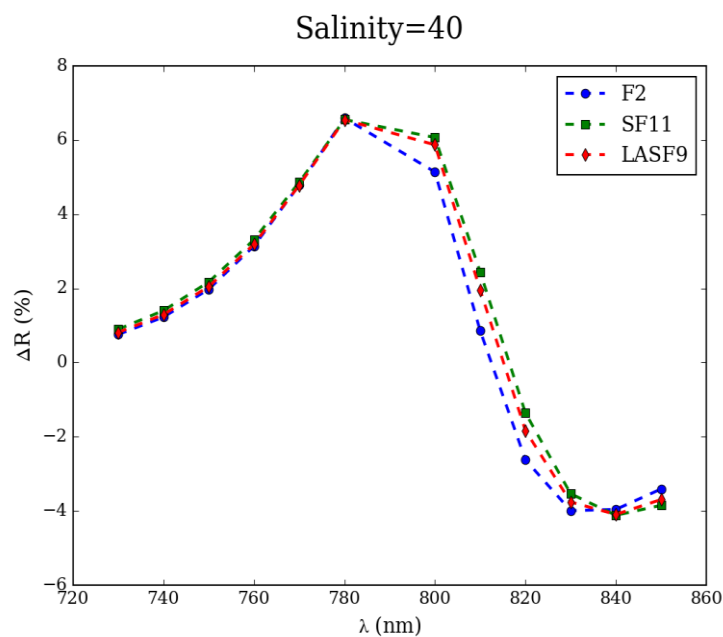


Figure 5.10: Reflectance change when the layer gets formed with regards to the illumination wavelength in the case of F2, SF11 and LASF9 prisms. The sample solvent is seawater of salinity 40.

Then we calculated the reflectance before and after a 1 nm thick layer of biomolecule gets immobilized on the SPR. The results are shown in Figure 5.7. As expected, when the molecules get adsorbed on the

surface, the resonance wavelength shifted to higher values. The total shift is about 4 nm in the three configurations.

Thereafter, the reflectance change for the 12 LED wavelengths was calculated. The results are plotted in Fig 5.8. The three configurations led to comparable results. The response slightly increases from F2 to SF11 and then LASF9. A maximum of 7% change can be expected with an illumination wavelength of 740 nm.

To consider the sample variability, the case of seawater of salinity 30 and 40 were also studied. The results are plotted in Fig 5.9 and 5.10, respectively. The resonance wavelength increases with the refractive index of the sample and then of the seawater practical salinity. The optimal LED wavelength had to be adjusted to 780 nm in these two cases. To conclude, the LED wavelength should range from about 730 to 800 to take into account the sample variability and the misalignment issues.

The material does not impact that much the response ( $\Delta R$ ) of the sensor. However, the angle of incidence depends strongly on it. The higher the refractive index, the lower the incidence angle is. In the case of SPRi, the sensor chip is imaged. The higher the image quality, the lower the incidence angle is. As a result, higher refractive index material should be preferred. F2 was then discarded. And as LASF9 is about 4 times more expensive than SF11, SF11 was chosen.

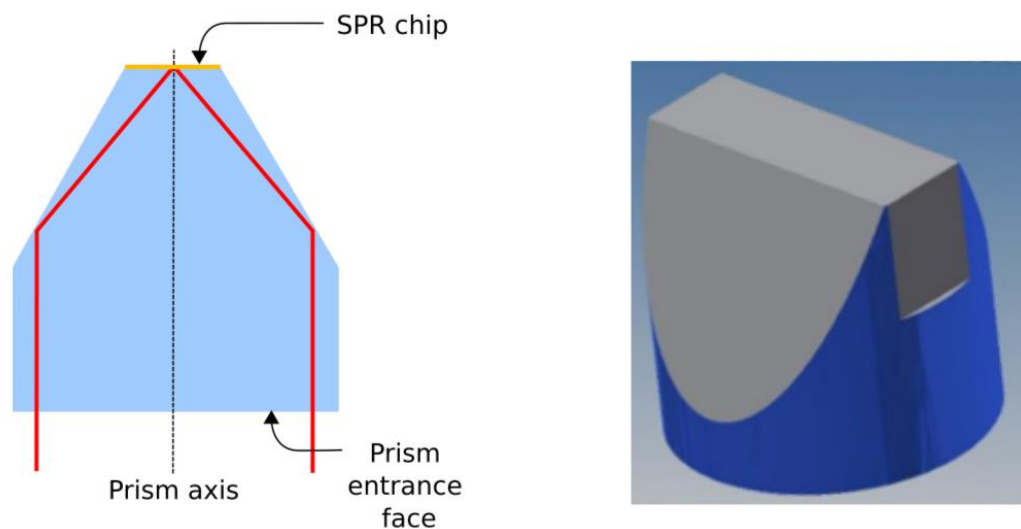


Figure 5.11: Prism geometry

The geometry of the prism can be shown of Fig 5.11. This geometry is similar to the geometry proposed by Cahill and co-workers (1997) and has previously been implemented into a marine sensor (Colas et al., 2016). The light beam gets into the prism and gets reflected by total internal reflection on the first glass/air interface. Thereafter, it is reflected on the gold interface. It is then reflected by TIR on the second glass/air interface and goes out of the prism. In this particular design, the light beam is aligned with the optical axis of the system as far as the entrance face of the prism is perpendicular to the optical bench. This particular configuration guarantees stable and easy alignment.

#### The flow cell:



The kinetics of the molecule reaction with the surface provides important data to SPRi system operators. A laminar flow is required in the flow cell. This leads to a particular design. The height of the flow cell should be chosen according to the flow rate. A typical height is 100  $\mu\text{m}$  for few mL/min flow rate.

An image of the SPRi chip is acquired by the camera. The active area is rectangular and its size is chosen relatively large to make the functionalization spotting convenient. Its dimension is of 10 mm length and 8 mm width.

#### The imaging system:

The lowest  $\sigma_{\text{min}}$  can be achieved for the highest signal-to-noise ratio (SNR) at the camera. In addition to measuring the slight changes, it is necessary to digitalize the signal with the largest possible bit depth. We therefore selected a 14-bits digital camera, the pixelfly-usb by PCO. It is uncooled because of cost efficiency considerations, but can grab frame with a readout noise as low as 6  $e^-$  rms and presents a SNR up to 68 dB.

The camera sensor is relatively large (9x6.7 mm). The magnification is then taken of 1.2 so that the image of the SPRi chip fills the camera sensor. The imaging optical system is then a pair of 50 mm and 60 mm lenses.

#### CAO of the SPRi sensor:

Based on the previous results a design of the SPRi sensor was proposed. It is shown on Fig 5.12 to 5.14. A relatively compact system was designed.

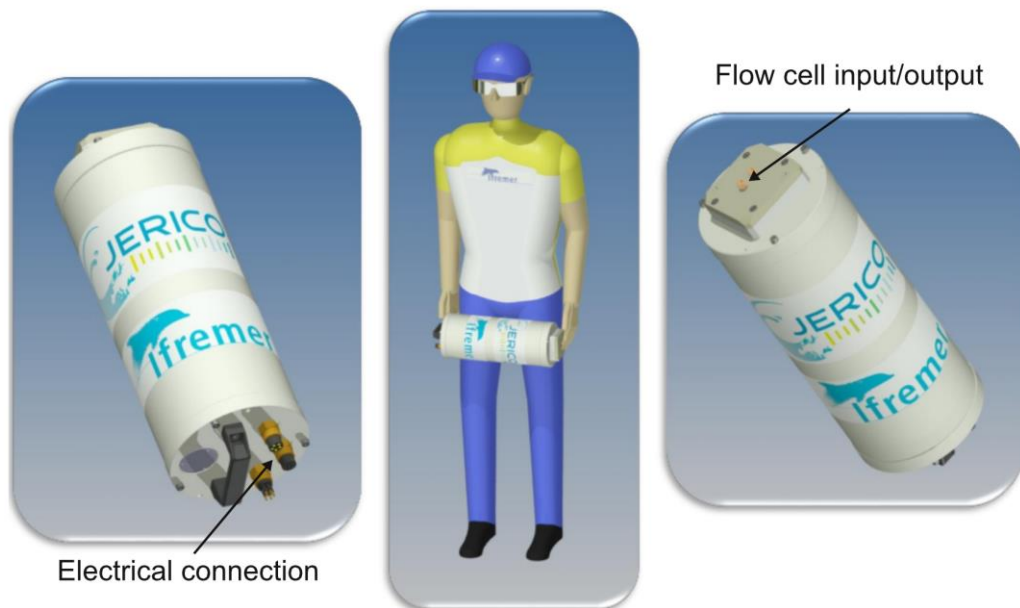
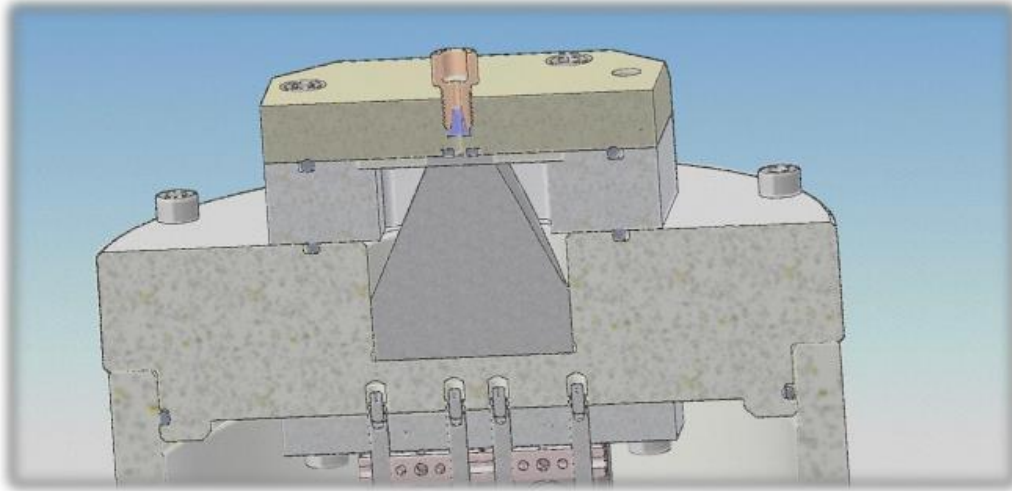
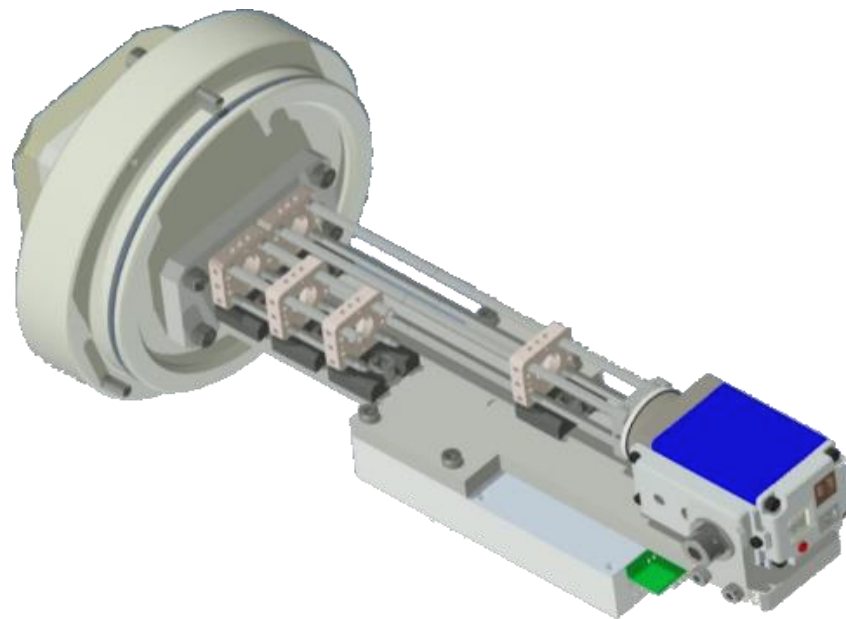


Figure 5.12: CAO of the SPRi sensor.



*The flow cell and prism side*

*Figure 5.13:*



*Figure 5.14: The optical bench.*

**Fluidic system:**

The fluidic system associated with the sensor is shown in Fig 5.15. It was previously developed for deep depth applications (Vuillemin et al., 2009). It consists of eight valves and three peristaltic pumps that can be turned clockwise and anticlockwise. The containers of reagent are stored in plastic bags and can be connected to any valves. This system offers robustness and versatility.



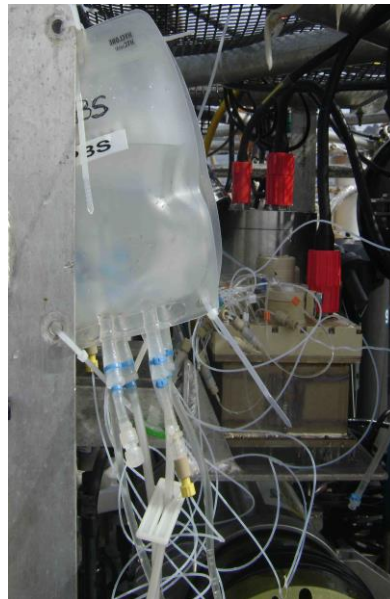


Figure 5.15: The fluidic module with reagent stored in plastic bags.

### 5.2.3 Detection protocol optimisation:

The typical detection strategy of an SPR sensor is to graft the specific receptor on the SPR chip and to detect the analyte bindings. Such a detection format is called *direct assay*. When dealing with a low molecular weight molecule (typically less than 1 kDa), this approach may not be sensitive enough. A classical strategy is the inhibition assay. In the context of this project, the receptor is a monoclonal antibody specific to DA.

Prior to the assay, the surface is functionalized with the DA. Then, the sample is mixed with the antibodies and the mixture incubates during a typical time of few hours. The mixture is then injected in the flow cell. The SPR signal is then proportional to the amounts of antibodies that did not bind to the DA in the sample (Figure 5.16). It is then inversely proportional to its concentration in the sample.

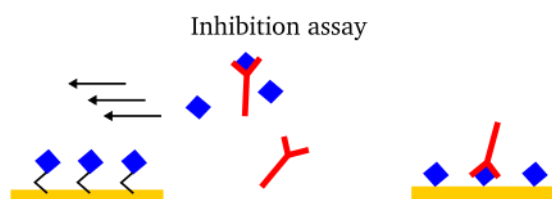


Figure 5.16: Inhibition assay

This kind of detection format was proven capable of detecting the toxin at concentration as low as 0.1ng/mL (Yu et al., 2005). It has already been used for *in situ* detection (Colas et al., 2016) during short term experiment. In the context of the JERICO-NEXT project, it had to be optimized for a 1-month duration deployment in coastal waters. In particular, the ageing of the chemicals and the reproducibility of the assay had to be improved. In addition, the impact of the temperature had to be characterized.

These studies were carried out with a laboratory SPR sensor (Reichert) and solutions of PBS spiked with DA.

### Reproducibility:

The deployment of the SPRi sensors requires the use of plastics manifolds and containers. The behaviour of the reagent in such containers had to be assessed. The plot of Fig 5.17 shows the response of the SPR system when the antibodies in PBS are stored in plastic vials. The signal varied with the number of measurement cycle. Different hypotheses was tested. The conclusion was that the reagent got adsorbed onto the plastic surface. The addition of a surfactant (Tween 20%) improved the ageing of the antibodies solutions in plastic containers.

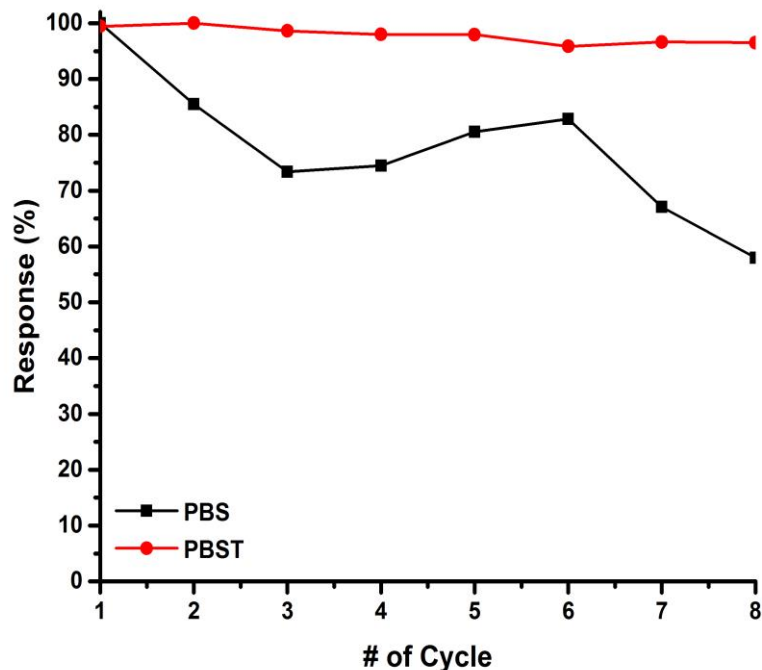


Figure 5.17: Relative response of the SPR chip when the antibodies are stored in PBS and PBS+Tween (PBST).

### Aging of the SPR chip:

The same chip was used about 100 times during 34 consecutive days. The signal showed a decrease of about 50%, but the correction by a reference signal was efficient. The sensor can still provide trustworthy measurement.

The next step will be to assess the ageing of the sensor and the reagents in mesocosm facilities. This will be carried out in 2018, when the new biosensor will have been fabricated and tested in the laboratory.

### Effect of the temperature:

To assess the effect of the temperature on the sensor, the detection assay was carried out in two different cases. The antibodies and the sample were first incubated at 4°, then at 20°. The responses of the SPR system are shown in Fig 5.18.

The two curves are similar, but the 4°C graph is translated toward smaller values leading to a lower EC50. Thus, the effect of the temperature has to be taken into account when analysing the data. A thermal regulation would be efficient, but is not adapted to *in situ* deployment. The strategy will be to fully characterise the effect of the temperature on the sensor and then to correct the data based on the temperature effect. This study will be carried on the final system in a thermoregulated bath facility at Ifremer.

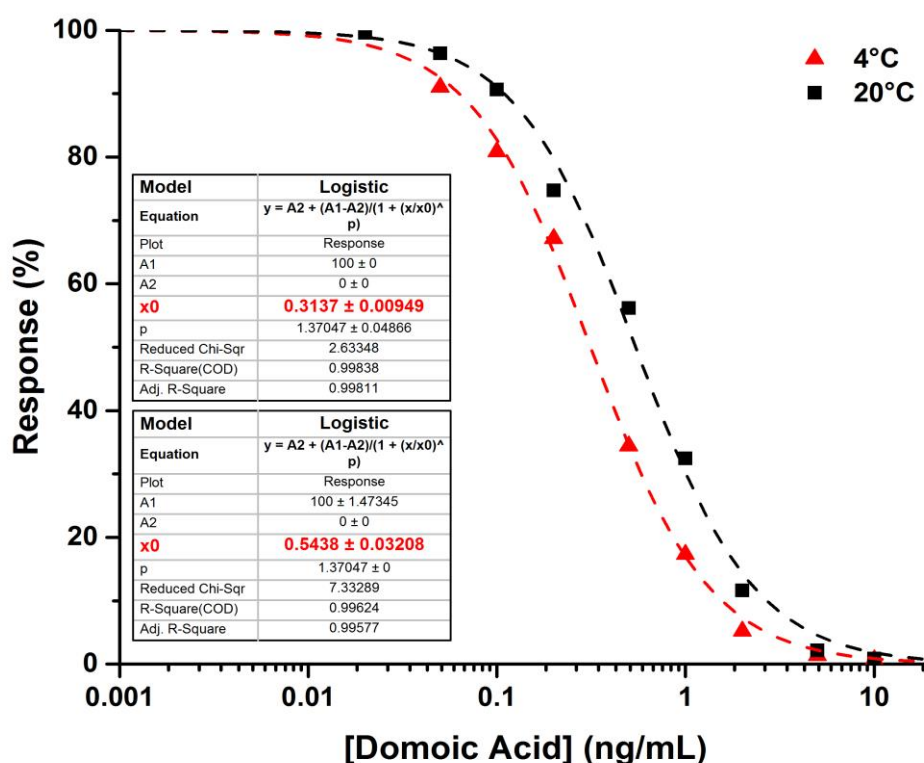


Figure 5.18: Response of the SPR sensor with regards to the DA concentration when the mixture incubates at 4 and 20°C.

The SPRi sensor has been optimized and designed. Within the next few months, it will be fabricated, assembled and tested in laboratory and mesocosm facilities. In addition, the ageing of the reagent was assessed and improved. However, most of the assays have been carried out with PBS solution spiked with DA. The next step will be to assess the protocol with seawater samples.



## 6 Preliminary conclusions and further work

Through Subtask 3.4.1, different assays for the quantification of key organisms for hydrocarbon pollution monitoring in marine coastal zones were tested and several markers from oil degrading organisms and genes involved in hydrocarbon degradation were selected for further work. Subtask 3.4.3 focused on developing a metabarcoding method for investigating biodiversity, comparing the results with data from more traditional methods. Through Subtasks 3.4.2, a new configuration was designed for the domoic acid biosensor. It enables the assay of several targets at the same time with reference measurements and replicates. The biosensor is first dedicated to this toxin, covering a concentration range from 0.1 to 2 ng/mL.

During the course of the next 12 months, the bacterial markers and assays will be tested in conjunction with WP4 JRAP3, during which a cruise has collected a series of samples which are being analysed for PHAs. Following this the microbial markers, algae sensor and domoic acid sensor will be tested through a series of environmental sampling campaigns to validated and integrate the results from the different biological sensors as well as chemical measurements. These will be performed during the next 24 months.

By the end of 2018, the domoic acid sensor will be tested in mesocosm facilities and then deployed on the Marel Iroise buoy in the Brest of Bay during the spring 2018. Two measurements of DA concentration per day will be carried out during one month.

After finalizing the development and tests of the DNA sensor for toxin algae through the EnviGuard project, the biosensor will be operated in combination with a stationary FerryBox and in the next step with an underway FerryBox system. First experiments will start at the earliest beginning of 2018 and will be continued until 2019. The timing of these investigations depends strongly on the successful final tests of the biosensor in the EnviGuard project. Main focus will be on the maturity of the biosensor in terms mechanical stability and the behaviour during unattended operation on a moving platform. Furthermore, the reliability of the obtained results will be investigated by bottle samples and microscopic evaluation.

The metabarcoding analysis will be performed on samples collected during the Tångesund study of phytoplankton biodiversity with a focus on harmful algae. 18S rDNA sequences obtained from natural populations will be compared to reference databases (PR2 and the new UniEuk database when available) to identify organisms when possible. The next step is to compare results from metabarcoding with imaging flow cytometry and microscopy.

The results of this Task will feed into WP1, WP2 and WP5, particularly during the final 12 months of the project.





## 7 References

- Abell G.C., Bowman J.P. (2005). Ecological and biogeographic relationships of class Flavobacteria in the Southern Ocean. *FEMS Microbiology ecology*, 1;51(2):265-77.
- Boccardo, C., Krolicka, A., Chevet, F., et al. (In prep). Migration of petroleum compounds from sea-ice into seawater and associated microbial community response during an *in situ* oil spill experiment in Svalbard (80°N).
- Boultart C., Mowlem M.C., Connelly D.P., et al. (2008). A novel, low-cost, high performance dissolved methane sensor for aqueous environments. *Optics Express*, 16(17):12607.
- Bru D., Sarr A., Philippot L. (2007). Relative Abundances of Proteobacterial Membrane-Bound and Periplasmic Nitrate Reductases in Selected Environments. *Applied and Environmental Microbiology*, 73:5971-5974.
- Cahill C.P., Johnston K.S., Yee S.S. (1997). A surface plasmon resonance sensor probe based on retro-reflection. *Sensors and Actuators B: Chemical*, 45(2):161–6.
- Campbell K., McGrath T., Sjölander S., et al. (2011). Use of a novel micro-fluidic device to create arrays for multiplex analysis of large and small molecular weight compounds by surface plasmon resonance. *Biosensors and Bioelectronics*, 26(6):3029–36.
- Colas F., Crassous M.P., Laurent S., et al. (2016). A surface plasmon resonance system for the underwater detection of domoic acid: Domoic Acid Detection Using SPR. *Limnology and Oceanography: Methods*, 14(7):456–65.
- de Vargas C., Audic S., Henry N., et al. (2015). Eukaryotic plankton diversity in the sunlit ocean. *Science*, 348 (6237).
- Deming J. W. (2002). Psychrophiles and polar regions. *Current Opinion in Microbiology* 3:301-309.
- Díaz-Herrera N., Esteban O., Navarrete M.C., et al. (2006). *In situ* salinity measurements in seawater with a fibre-optic probe. *Measurement Science and Technology*, 17(8):2227.
- Diercks S., Metfies K., and Medlin L.K. (2008). Development and adaptation of a multiprobe biosensor for the use in a semi-automated device for the detection of toxic algae, *Biosensors and Bioelectronics*, 23, 1527–1533.
- Edvardsen B., Dittami S.M., Groben R., et al. (2013). Molecular probes and microarrays for the detection of toxic algae in the genera *Dinophysis* and *Phalacroma* (Dinophyta). *Environmental Science and Pollution Research*, 20:6733-6750
- Egge E., Bittner L., Andersen T., et al. (2013). 454 Pyrosequencing to Describe Microbial Eukaryotic Community Composition, Diversity and Relative Abundance: A Test for Marine Haptophytes. *PLOS ONE* 8:e74371.
- Fitzpatrick E., Caron D.A., Schnetzer A. (2010). Development and environmental application of a genus-specific quantitative PCR approach for *Pseudo-nitzschia* species. *Marine Biology*. (157), 1161-1169.
- Gobi K.V., Miura N. (2004). Highly sensitive and interference-free simultaneous detection of two polycyclic aromatic hydrocarbons at parts-per-trillion levels using a surface plasmon resonance immunosensor. *Sensors and Actuators B: Chemical*, 103(1–2):265–71.





- Guy C.J., Bowman J.P. (2005). Ecological and biogeographic relationships of class Flavobacteria in the Southern Ocean. *FEMS Microbiology*, (51):265-277.
- Harris R., Luff B., Wilkinson J., et al. (1999). Integrated optical surface plasmon resonance immunoprobe for simazine detection. *Biosensors and Bioelectronics*, 14(4):377–86.
- Henry S., Bru D., Stres B., et al. (2006). Quantitative Detection of the *nosZ* Gene, Encoding Nitrous Oxide Reductase, and Comparison of the Abundances of 16S rRNA, *narG*, *nirK* and *nosZ* Genes in Soils. *Applied Environmental Microbiology*, 72(8):5181-5189.
- Homola J. (2006). *Surface Plasmon Resonance Based Sensors*. Berlin, Heidelberg: Springer-Verlag Berlin Heidelberg.
- Hu Y.O.O., Karlson B., Charvet S., Andersson A.F. (2016). Diversity of Pico- to Mesoplankton along the 2000 km Salinity Gradient of the Baltic Sea. *Frontiers in Microbiology*, 7:679.
- Karlson B., Andersson L.S., Kaitala S., et al. (2016). A comparison of FerryBox data vs. monitoring data from research vessels for near surface waters of the Baltic Sea and the Kattegat. *Journal of Marine Systems*, 162:98-111.
- Karlson B., Cusack C., Bresnan E. (2010). Microscopic and molecular methods for quantitative phytoplankton analysis. *Intergovernmental Oceanographic Commission manuals and guides*.
- Kegel J.U., Guillebault D., Medlin L.K. (2016). Application of microarrays (phylochips) for analysis of community diversity by species identification. *Perspectives in Phycology*, 93-106.
- Kim Y-C., Cramer J.A., Booksh K.S. (2011). Investigation of a fiber optic surface plasmon spectroscopy in conjunction with conductivity as an *in situ* method for simultaneously monitoring changes in dissolved organic carbon and salinity in coastal waters. *Analyst journal*, 136(20):4350–6.
- Kirchman D.L. (2002). The ecology of *Cytophaga-flavobacterium* in aquatic environments. *FEMS Microbiology ecology*, 39:91-100.
- Knapik K, 2017 (unpublished results)
- Krolicka A., Boccadoro C., Maeland M., Baussant T. (2014). Detection of oil leaks by quantifying hydrocarbonoclastic bacteria in cold marine environments using the Environmental Sample Processor. *Proceedings of the 37th AMOP Technical Seminar on Environmental Contamination and Response*.
- Kwok L-Y., Zhang J., Guo Z., et al. (2014). Characterization of Fecal Microbiota across Seven Chinese Ethnic Groups by Quantitative Polymerase Chain Reaction. *PLoS ONE* 9(4): e93631.
- Lang T., Hirsch T., Fenzl C., et al. (2012). Surface Plasmon Resonance Sensor for Dissolved and Gaseous Carbon Dioxide. *Analytical Chemistry*, 84(21):9085–8.
- Lotierzo M., Henry O.Y., Piletsky S., et al. (2004). Surface plasmon resonance sensor for domoic acid based on grafted imprinted polymer. *Biosensors and Bioelectronics*, 20(2):145–52.
- Maillart E. (2004). Développement d'un système optique d'imagerie en résonance de plasmons de surface pour l'analyse simultanée de multiples interactions biomoléculaires en temps réel. [Orsay]: Université Paris XI.





- Mason O.U., Hazen T.C., Borglin S., et al. (2012). Metagenome, metatranscriptome and single-cell sequencing reveal microbial response to Deepwater Horizon oil spill. *ISME Journal*, 6:1715–1727.
- McNamee S.E., Elliott C.T., Delahaut P., Campbell K. (2013). Multiplex biotoxin surface plasmon resonance method for marine biotoxins in algal and seawater samples. *Environmental Science and Pollution Research*, 20(10):6794–807.
- Medlin L. (2016). Mini Review: Molecular Techniques for Identification and Characterization of Marine Biodiversity. *Annals of Marine Biology and Research* 3.
- Metfies, K., Schroeder F., Hessel J., et al. (2016). High-resolution monitoring of marine protists based on an observation strategy integrating automated on-board filtration and molecular analyses, *Ocean Science.*, 12:1237-1247.
- Meyer A., Todt C., Mikkelsen N. T. & Lieb B. (2010). "Fast evolving 18S rRNA sequences from Solenogastres (Mollusca) resist standard PCR amplification and give new insights into mollusk substitution rate heterogeneity". *BMC Evolutionary Biology* 10: 70. doi:10.1186/1471-2148-10-70
- Minunni M., Mascini M. (1993). Detection of Pesticide in Drinking Water Using Real-Time Biospecific Interaction Analysis (BIA). *Analytical Letters*, 26(7):1441–60.
- Nadkarni M.A., Martin F.E., Jacques N.A., Hunter N. (2002). Determination of bacterial load by real-time PCR using a broad-range (universal) probe and primer set. *Microbiology*, 148, 257-66.
- Nubel U., Garcia-Pichel F., Muyzer G. (1997). PCR Primers to amplify 16S rRNA genes from cyanobacteria. *Applied Environmental Microbiology*, (63):3327–3332.
- Ock K., Jang G., Roh Y., et al. (2001). Optical detection of Cu<sup>2+</sup> ion using a SQ-dye containing polymeric thin-film on Au surface. *Microchemical Journal*, 70(3):301–5.
- Poly P., Ranjard L., Nazaret S., et al. (2001). Comparison of NifH gene pools in soils and soil microenvironments with contrasting properties. *Applied Environmental Microbiology*, 67(5):2255-2262.
- Redmond M. C., Valentine D. L. (2012). Natural gas and temperature structured a microbial community response to the Deepwater Horizon oil spill. *Proceedings of the National Academy of Science U.S.A.*, 109;20292–20297.
- Rotthauwe J.H., Witzel K.P., Liesack W. (1997). The ammonia monooxygenase structural gene amoA as a functional marker: molecular fine-scale analysis of natural ammonia-oxidizing populations. *Applied Environmental Microbiology*, 63:4704–4712.
- Takai K., Horikoshi K. (2000). Rapid detection and quantification of members of the archaeal community by quantitative PCR using fluorogenic probes. *Applied and Environmental Microbiology*, (66):5066-5072.
- Vuillemin R., Le Roux D., Dorval P., et al. (2009). CHEMINI: A new in situ CHEmical MINIaturized analyzer. *Deep Sea Research Part I: Oceanographic Research Papers*, 56(8):1391–9.
- Wu C-M, Lin L-Y. (2004). Immobilization of metallothionein as a sensitive biosensor chip for the detection of metal ions by surface plasmon resonance. *Biosensors and Bioelectronics*, 20(4):864–71.
- Woese CR, Fox GE (1977). Phylogenetic structure of the prokaryotic domain: the primary kingdoms. *Proceedings of the National Academy of Sciences of the United States of America*. 74 (11): 5088–90. Bibcode:1977PNAS...74.5088W. PMC 432104. PMID 270744. doi:10.1073/pnas.74.11.5088.





Woese CR, Kandler O, Wheelis ML (1990). Towards a natural system of organisms: proposal for the domains Archaea, Bacteria, and Eucarya". *Proceedings of the National Academy of Sciences of the United States of America*. **87** (12): 4576–9. Bibcode:1990PNAS...87.4576W. PMC 54159. PMID 2112744. doi:10.1073/pnas.87.12.4576.

Yakimov M.M., Giuliano L., Gentile G. et al. (2003). *Oleispira antarctica* gen. nov., sp. Nov., a novel hydrocarbonoclastic marine bacterium isolated from Antarctic coastal sea water. *International Journal of Systematic Evolutionary Microbiology*, 53:779-85.

Yu Q., Chen S., Taylor A.D., et al. (2005). Detection of low-molecular-weight domoic acid using surface plasmon resonance sensor. *Sensors and Actuators B: Chemical*, 107(1):193–201.

